# Strain Promoted Click Chemistry of 2- or 8-Azidopurine and 5-Azidopyrimidine Nucleosides and 8-Azidoadenosine Triphosphate with Cyclooctynes. Application to Living Cell Fluorescent Imaging

Jessica Zayas,[†] Marie Annoual,[†] Jayanta Kumar Das,[‡] Quentin Felty,[‡] Walter G. Gonzalez,[†] Jaroslava Miksovska,[†] Nima Sharifai,[§] Akira Chiba,[§] and Stanislaw F. Wnuk*[,†,‡]

[†]Department of Chemistry and Biochemistry and [‡]Department of Environmental and Occupational Health, Florida International University, Miami, Florida 33199, United States

[§]Department of Biology, University of Miami, Coral Gables, Florida 33146, United States

Ⓢ *Supporting Information*

**ABSTRACT:** Strain-promoted click chemistry of nucleosides and nucleotides with an azido group directly attached to the purine and pyrimidine rings with various cyclooctynes in aqueous solution at ambient temperature resulted in efficient formation (3 min to 3 h) of fluorescent, *light-up*, triazole products. The 2- and 8-azidoadenine nucleosides reacted with fused cyclopropyl cyclooctyne, dibenzylcyclooctyne, or monofluorocyclooctyne to produce click products functionalized with hydroxyl, amino, *N*-hydroxysuccinimide, or biotin moieties. The 5-azidouridine and 5-azido-2′-deoxyuridine were similarly converted to the analogous triazole products in quantitative yields in less than 5 min. The 8-azido-ATP quantitatively afforded the triazole product with fused cyclopropyl cyclooctyne in aqueous acetonitrile (3 h).



Fluorescent Imaging in Live Cancer Cells

FD-FLIM in Live Cancer Cells

The novel triazole adducts at the 2- or 8-position of adenine or 5-position of uracil rings induce fluorescence properties which were used for direct imaging in MCF-7 cancer cells without the need for traditional fluorogenic reporters. FLIM of the triazole click adducts demonstrated their potential utility for dynamic measuring and tracking of signaling events inside single living cancer cells.
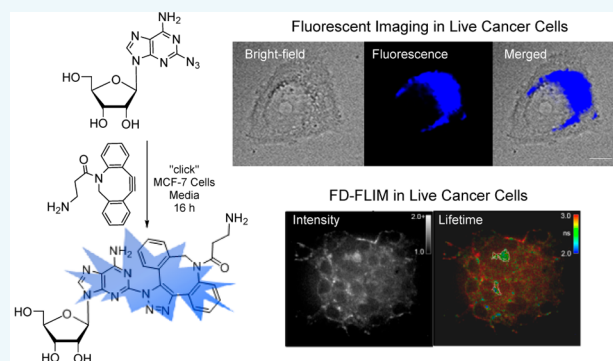
## INTRODUCTION

Click chemistry is a common method used for drug discovery, bioconjugation, proteomic profiling, and potential identification of cellular targets.[1−3] The strain promoted 1,3-dipolar [3 + 2] cycloaddition of azides and cyclooctyne (SPAAC) derivatives, first discovered by Bertozzi[4−8] and further developed by Boons[9] and van Delft,[10−12] occurs readily under physiological conditions in the absence of supplementary reagents such as copper and microwave heating. The SPAAC reactions are also used for the selective modification of compounds or living cells[7,13] including for the imaging of cell surface glycoproteins by fluorescence lifetime imaging microscopy.[14]

Nucleosides, nucleotides, and oligonucleotides have now been explored as substrates for click chemistry for some time.[15−17] Bioconjugation of nucleosides and oligonucleotides bearing alkyne modified nucleobases with azide modified fluorescent dyes, sugars, and peptides have been well documented.[2,16−19] These coupling reactions usually required Cu(I), a ligand, and heating or overnight stirring. Click chemistry of nucleosides and oligodeoxynucleotides (ODNs) with modified sugars bearing terminal alkyne groups have been also explored.[15,17,20−23]
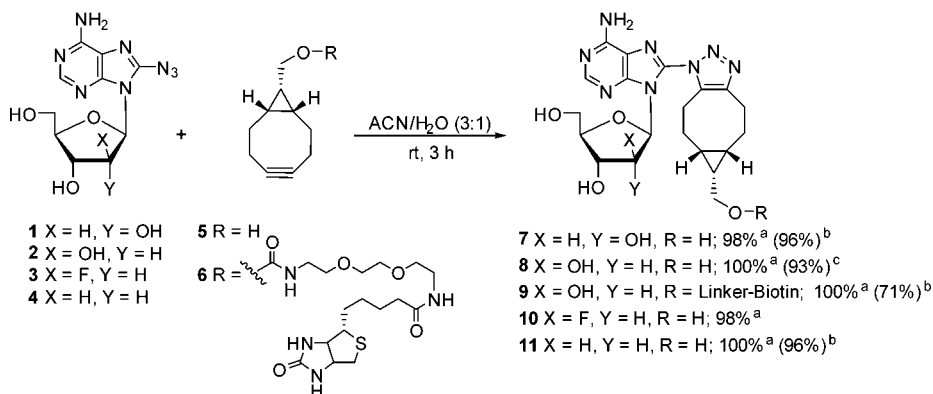
Azide modified sugars,[24−28] such as AZT, have also been studied in click chemistry with typical reaction conditions including the addition of Cu(I) and/or microwave assisted heating. However, the application of the nucleosides bearing an azido group attached directly to the heterocyclic bases in the click chemistry with alkyne partners has received much less attention thus far. This is due to the less developed chemical[28−34] and enzymatic[35−37] synthesis of azido nucleosides and oligonucleotides and their *apparent* lack of compatibility with the solid-phase synthesis of DNA fragments which required trivalent phosphorus-based precursors.[38] Furthermore, Cu⁺/Cu²⁺ ions often used for click chemistry are known to mediate DNA cleavage.[39]

The 8-azidoadenosine was found to be unreactive with terminal alkyne bearing cyclen Eu³⁺ complexes even after prolonged reaction times (120 h), addition of a large excess of CuSO₄·5H₂O, sodium ascorbate, and refluxing in DMF.[40] The ribose protected 8-azidoadenosine afforded, however, triazole product in modest yields when treated with (trimethylsilyl)-acetylene at 80 °C for 20 h.[41] Similarly, the 2-azidopurine

**Scheme 1. Strain Promoted Click Chemistry of 8-Azidoadenine Nucleosides**



1 X = H, Y = OH    5 R = H

2 X = OH, Y = H    6 R =

3 X = F, Y = H

4 X = H, Y = H

7 X = H, Y = OH, R = H; 98%[a] (96%)[b]

8 X = OH, Y = H, R = H; 100%[a] (93%)[c]

9 X = OH, Y = H, R = Linker-Biotin; 100%[a] (71%)[b]

10 X = F, Y = H, R = H; 98%[a]

11 X = H, Y = H, R = H; 100%[a] (96%)[b]

[a]Based on ^{1}H NMR. [b]Purified by RP HPLC. [c]Purified on silica gel column.

nucleosides were only moderately reactive in copper catalyzed click reactions[42−44] and also required several equivalents of alkyne and prolonged reaction times. These prerequisites are, however, unsuitable for biological applications including the potential medicinal applications because of the harsh conditions used and cytotoxic effect of the copper catalyst.[45,46] Moreover, the coupling between 5-azidouridine analogues and terminal alkynes are also scarcely developed,[47] mainly because of the photochemical instability of the 5-azidouracil substrates.[48] To overcome these limitations, the 5-(azido)methyluracil nucleosides were used instead to study the click chemistry of azido-modified pyrimidine bases.[49] Furthermore, the strain promoted click chemistry with cyclooctyne modified phosphate backbone for labeling of DNA[50−52] and RNA[39,53] has recently been developed.[54]

Naturally occurring nucleic acid components are usually nonfluorescent; therefore, fluorescence has typically been conferred on nucleosides by extending π conjugation of the heterocyclic base[55,56] or by conjugation with known fluorophores.[57,58] Herein, we report a protocol for the convenient strain promoted click chemistry (SPAAC) of 2- or 8-azidoadenine and 5-azidouracil nucleosides and 8-azidoadenosine triphosphate with various cyclooctynes in aqueous solution at ambient temperature and its application to imaging in living cells by *direct* fluorescence light-up.

## RESULTS AND DISCUSSION

**Synthesis.** Reaction between the equivalent amounts of 8-azidoadenosine[59] 1 and symmetrically fused cyclopropyl cyclooctyne[10] (OCT) 5 occurred efficiently in an aqueous solution of acetonitrile (ACN) at ambient temperature (3 h) to produce triazole 7 in 96% yield as a mixture[60] of ~1:1 regioisomers after silica gel chromatography or HPLC purification (Scheme 1). This reaction time and efficiency were similar when coupling of 1 and 5 was carried out in MeOH, EtOH, or Opti-MEM I cell culture media (see Table S1 in SI for reaction details). A kinetic analysis of the click reaction between azide 1 and cyclooctyne 5 showed that reaction occurred rapidly (60% conversion in 20 min) without the formation of any byproducts (Figure 1). The profile for the reaction was measured by integrating disappearance of the signal of H2 of substrate 1 at 8.07 ppm and appearance of H2 signal at 8.28 ppm for the product 7 on ^{1}H NMR spectra. This reaction displays a second-order rate constant of 0.11 M^{−1} s^{−1} which is similar to the previously published data on the reaction
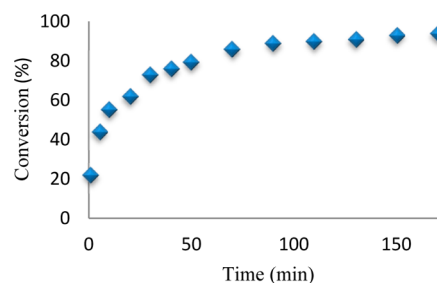


**Figure 1.** Kinetic profile of the SPAAC reaction of the equivalent amount of 8-azidoadenosine 1 and cyclooctyne 5 in ACN-$d_6$/D$_2$O (3:1, v/v; 23 mM) as monitored by ^{1}H NMR.
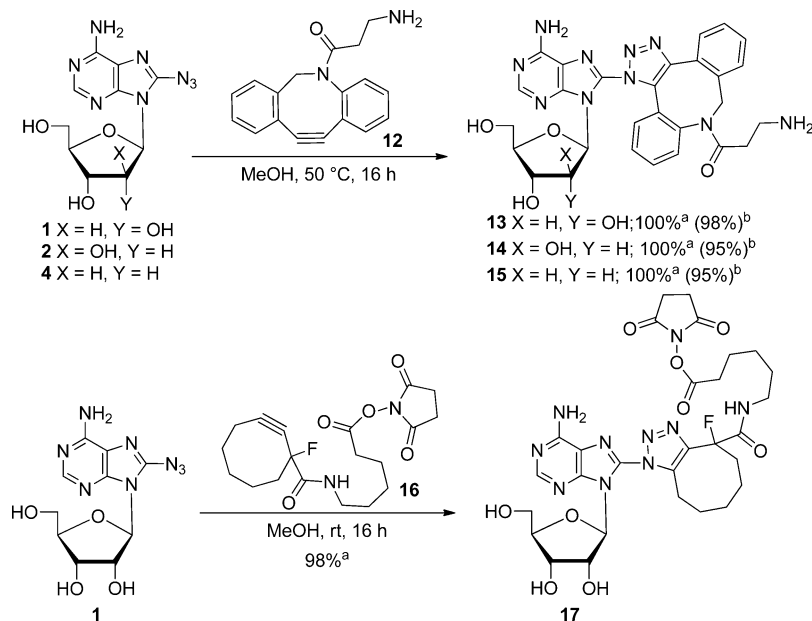
of 5 with benzyl azide in the same solvent system ($k$ = 0.14 M^{−1} s^{−1})[10] (see SI for more details).

The reaction between 8-azido-9-($\beta$-D-arabinofuranosyl)-adenine[61] 2 or 8-azido-9-(2-deoxy-2-fluoro-$\beta$-D-arabinofuranosyl)adenine 3 (see SI for the synthesis of 3) and cyclooctyne 5 also proceeded smoothly (3 h, rt) in ACN/H$_2$O (3:1) to give triazole 8 or 10, quantitatively. Analogous treatment of 8-azido-2′-deoxyadenosine[62] 4 with 5 gave the click product 11 (96%). Since biotin tagging is a common in vivo method used for visualization of proteins and biomolecules with streptavidin, we also demonstrated quantitative labeling of azide 2 with biotin modified OCT 6 to give labeled adduct 9.

The click reaction of 1 with more complex cyclooctynes including strain modulated dibenzylcyclooctyne[63] (DBCO) 12 or electronic modulated monofluorocyclooctyne[64,65] (MFCO) 16 in polar protic solvents produced the triazoles modified with a terminal amine 13 or "reactive" N-hydroxysuccinimide ester 17, quantitatively as 1:1 mixture of isomers (Scheme 2). The reaction of 1 with 12 required overnight heating at 50 °C, while coupling of 1 and 16 was completed at ambient temperature overnight. Goddard and Bertozzi noted that although the aryl ring fusion may enhance the cyclooctyne ring stain, the sluggish reactivity of DBCO 12 with azides can be attributed to the "flagpole" hydrogen atoms ortho to the aryl/cyclooctyne ring junction which decrease reactivity by steric interference with the azide in the transition state.[8,66] Furthermore, azido nucleosides 2 and 4 react with 12 to give the corresponding triazole products 14 and 15, respectively.

The 2-azidoadenosine 19 also undergoes SPAAC reaction efficiently (Scheme 3). Thus, 19 reacts with cyclooctyne 5 in aqueous media at ambient temperature (3 h) to yield adduct 18 in quantitative yield. Similarly, 19 reacts with 12 to afford

**Scheme 2. Strain Promoted Click Chemistry of 8-Azidoadenine Nucleosides with Dibenzyl or Monofluoro Cyclooctyne**



1 X = H, Y = OH
2 X = OH, Y = H
4 X = H, Y = H

13 X = H, Y = OH; 100%[a] (98%)[b]
14 X = OH, Y = H; 100%[a] (95%)[b]
15 X = H, Y = H; 100%[a] (95%)[b]

MeOH, 50 °C, 16 h

MeOH, rt, 16 h
98%[a]

[a]Based on ^{1}H NMR. [b]Purified by RP HPLC.

**Scheme 3. Strain Promoted Click Chemistry of 2-Azidoadenosine**



18

ACN/H₂O (3:1)
rt, 2 h
100%[a]

19

MeOH, 50 °C, 16 h
98%[a], 85%[b]

20
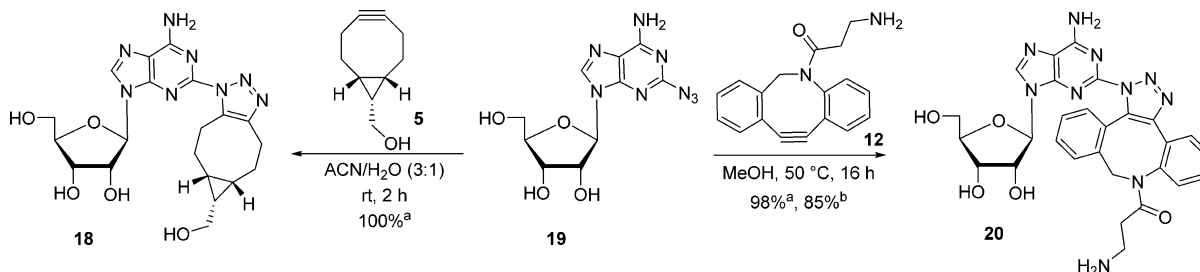
[a]Based on ^{1}H NMR. [b]Purified by RP HPLC.

triazole **20** but, as also noted above (Scheme 2), elevated temperature (50 °C) was required for the completion. The natural and 2-substituted purine nucleosides and nucleotides favor an *anti*-glycosyl bond orientation;[67] however, addition of bulky substituents at the C8 position forces a predominantly *syn* conformation in solution because of the unfavorable steric and electrostatic repulsions between the 8-substituent and the ribose ring.[68,69] Thus, the C2 and C8 modified click adducts described here provide analogues with both *syn*- and *anti*-conformations offering the potential for differing cellular targets.
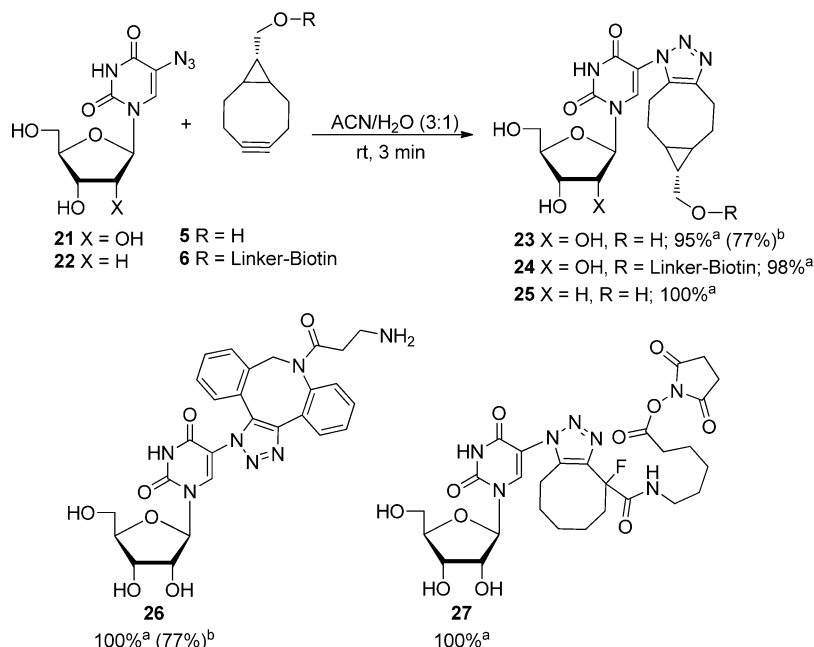
The click reaction between 5-azidouridine[47] **21** and several cyclooctynes including **5**, **6**, **12**, or **16** also proceeded efficiently yielding the corresponding novel click adducts **23**, **24**, **25**, and **27**. Thus, treatment of **21** with hydroxyl or biotin modified cyclooctyne **5** or **6** in ACN:H₂O mixture (3:1, v/v) afforded **23** or **24** in as fast as 3 min at ambient temperature (Scheme 4). Analogous treatment of **21** with free amine modified dibenzylcyclooctyne **12** or NHS modified monofluorocyclooctyne **16** in MeOH gave complete conversion to triazoles **26** or **27** in less than 15 min. Furthermore, click reaction of the highly photolyzable 5-azido-2′-deoxyuridine[70] **22** with cyclooctyne **5**, in the ACN/H₂O/MeOH (3:1:1 v/v/v), provided corresponding triazole product **25** in excellent yield. The latter coupling

must be run in the dark in order to avoid the known photolysis of **22** caused by UV irradiation.[48] Substrate **22** was prepared by conversion of 5-bromo-2′-deoxyuridine[71] to 5-amino derivative followed by Sandmeyer azidation.[70]

Since click chemistry for labeling oligonucleotides are an emerging field,[28,31−33] we established a protocol for SPAAC with azido base modified nucleotides. Thus, reaction of 8-azidoadenosine 5′-triphosphate tetralithium salt **28** and cyclooctyne **5** in aqueous ACN (3 h) quantitatively yielded triazole **29** (Scheme 5). A kinetic analysis of this reaction depicted in Figure 2 shows that reaction occurred efficiently (55% in 35 min, 92% in 2 h) without formation of byproducts. This reaction displays a second-order rate constant of 0.07 $M^{-1}$ $s^{-1}$, which is similar to the previously published data on reaction of **5** with benzyl azide in the same solvent system[10] (see SI for more details).

In summary, the efficiency of the SPAAC reaction between azido nucleosides and cyclooctynes strongly depends on the structure of azido and cyclooctyne substrates, whereas the choice of the solvent has less effect. Thus, the 5-azidouracil precursors were significantly more reactive than the 2- or 8-azidoadenine substrates; however, the position of the azido group on the adenine scaffold did not affect reactivity of adenine substrates. As cyclooctynes are concerned, the OCT **5**

**Scheme 4. Strain Promoted Click Chemistry of 5-Azidouridine and 5-Azido-2′-deoxyuridine**



21 X = OH
22 X = H

5 R = H
6 R = Linker-Biotin

23 X = OH, R = H; 95%[a] (77%)[b]
24 X = OH, R = Linker-Biotin; 98%[a]
25 X = H, R = H; 100%[a]

26
100%[a] (77%)[b]

27
100%[a]

[a]Based on ^{1}H NMR. [b]Purified by RP HPLC.

**Scheme 5. Strain Promoted Click Chemistry of 8-Azidoadenosine 5′-triphosphate 28**
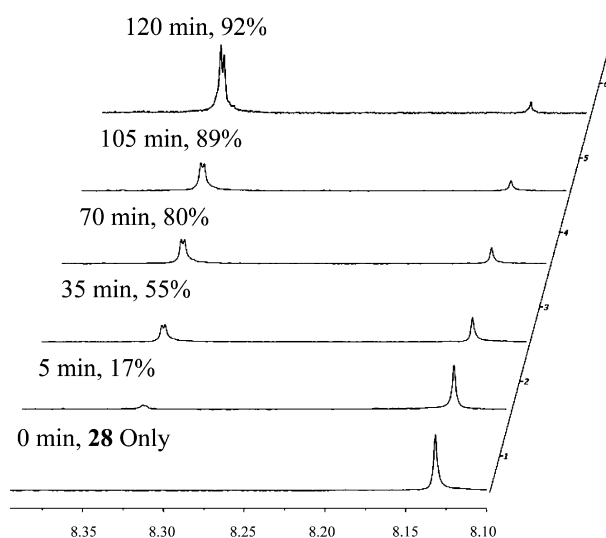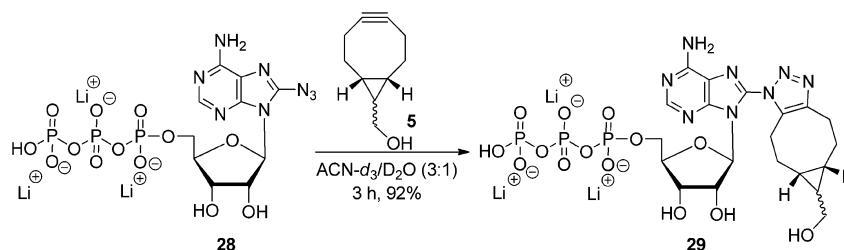


28

29



**Figure 2.** Kinetic profile of the reaction between azidonucleotide **28** and cyclooctyne **5** in ACN-$d_6$/D$_2$O (3:1, v/v; 6 mM) as monitored by ^{1}H NMR.

appeared to be the most reactive toward azido nucleosides followed by MFCO **16** and last DBCO **12** (see Table S1 in SI for a summary of reaction conditions and yields). The selection

of solvents for the click reactions was based on substrate solubility. For example, some azido nucleosides (e.g., **1** or **2**) are water-soluble, while others are not (e.g., **22**) and require methanol to solubilize. Also, the hydrocarbon scaffold of the cyclooctynes limits their solubility in aqueous solutions.[72] Typical SPAAC reactions for the uridine substrate **21** with OCT **5**, MFCO **16**, or DBCO **12** were completed in 5 min (rt), 12 min (rt), and 15 min (rt), respectively; whereas reactions for the adenosine substrate **1** with the same cyclooctynes required 3 h (rt), 16 h (rt), and 16 h (50 °C), respectively, in aqueous ACN or MeOH.

**Fluorescent Characterization.** Unsubstituted nucleosides are typically weakly fluorescent;[73−76] however, substitution at the C2 and C8 position of the purine ring or C5 of the pyrimidine ring with fluorogenic moieties results in nucleosides with fluorescent properties.[19,77,78] While the 8-azido-*arabino*-adenosine **2** has no fluorescence, the click adduct **7** with triazole ring attached *directly* to the imidazolyl ring of purine via a nitrogen atom emits at 300−500 nm with the maximum emission at 376 nm ($\Phi_{em}$ = 0.6%, B = 0.13 M$^{-1}$ cm$^{-1}$). Similarly, 5-azidouridine **21** exhibits no noticeable fluorescence, whereas the triazole product **23** shows moderate emission between 285 and 550 nm with two emission peaks at 324 and 440 nm ($\Phi_{em}$ = 1.1%, B = 0.12 M$^{-1}$ cm$^{-1}$). Interestingly, this triazole product showed an excitation maxima at 388 nm which
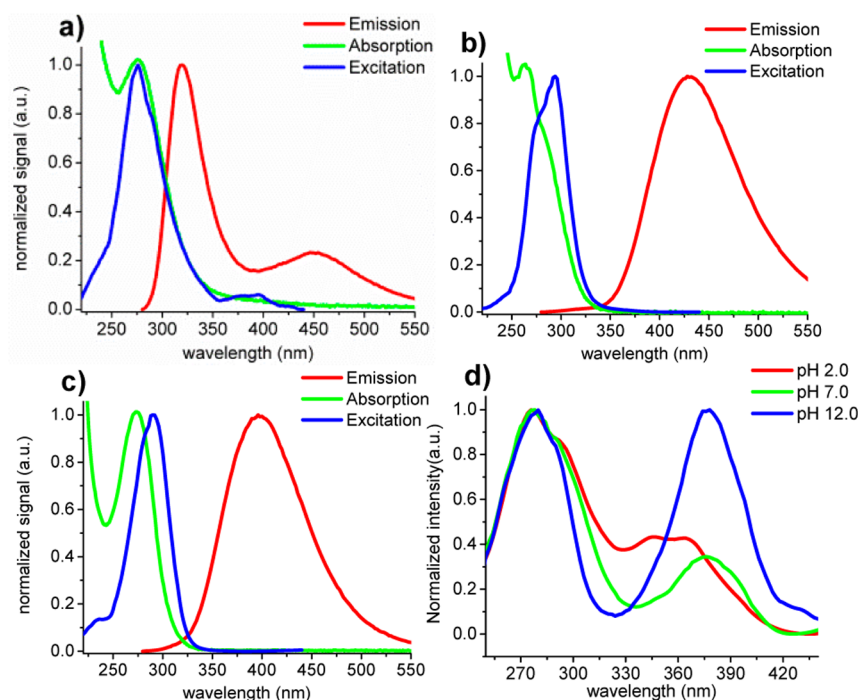
**Figure 3.** Normalized fluorescence emission, absorption, and excitation spectra for the selected click adducts: (a) **23**, (b) **11**, and (c) **20** in MeOH; (d) pH effect on the excitation spectra of **23** in phosphate buffer.

### Table 1. Photophysical Data for the Selected Triazole Adducts

|  | 7 | 8 | 11 | 13 | 17 | 18 | 20 | 23 | 26 | 27 |
|---|---|---|---|---|---|---|---|---|---|---|
| $\varepsilon_{max}$ (M$^{-1}$ cm$^1$) | 21100 | 17500 | 18200 | 16000 | 16400 | 19100 | 16400 | 10100 | 7300 | 7100 |
| $\lambda_{max}$ (abs)$^a$ (nm) | 270 | 273 | 272 | 276 | 271 | 261 | 263 | 270 | 276 | 269 |
| $\lambda_{max}$ (exc)$^a$ (nm) | 280 | 278 | 290 | 293 | 288 | 270 | 295 | 276 | 312 | - |
| $\lambda_{max}$ (exc)$^{a,d}$ (nm) | 309 | - | - | 360 | - | 329 | - | 388 | 370 | - |
| $\lambda_{max}$ (emi)$^a$ (nm) | 392 | 390 | 397 | 440 | 399 | 395 | 428 | 312 | 361 | 327/412 |
| $\lambda_{max}$ (emi)$^b$ (nm) | 376 | 384 | 392 | 429 | 397 | 375 | 422 | 324/440 | - | 331/419 |
| $\lambda_{max}$ (emi)$^c$ (nm) | 403 | 400 | 402 | 452 | 399 | 405 | 439 | 334/445 | - | 339/434 |
| Stokes shift$^a$ (nm) | 83 | 112 | 107 | 80 | 111 | 66 | 133 | 44/62 | 49 | 58 |
| $\Phi_F{}^a$ | 0.006 | 0.006 | 0.014 | 0.017 | 0.006 | 0.02 | 0.106 | 0.011 | 0.013 | 0.009 |
| brightness$^a$ (M$^{-1}$ cm$^1$) | 0.13 | 0.11 | 0.25 | 0.27 | 0.10 | 0.38 | 1.74 | 0.12 | 0.09 | 0.06 |
| $\tau_1{}^a$ (ns) | 0.10 | 0.60 | 0.10 | - | 0.10 | 0.30 | 0.10 | 0.30 | 0.30 | - |
| $\tau_2{}^a$ (ns) | 0.80 | 4.90 | 0.90 | - | 0.90 | 1.0 | 2.0 | 1.30 | 2.30 | - |
| $\tau_3{}^a$ (ns) | 5.90 | - | 5.60 | - | 5.30 | 5.80 | 4.10 | 5.70 | 7.80 | - |
| $\tau_{average}$ (ns) | 0.70 | 1.60 | 1.60 | - | 1.20 | 0.80 | 2.80 | 2.70 | 2.70 | - |
| $f_1{}^a$ (%) | 0.63 | 0.77 | 0.28 | - | 0.46 | 0.64 | 0.02 | 0.22 | 0.11 | - |
| $f_2{}^a$ (%) | 0.30 | 0.23 | 0.53 | - | 0.39 | 0.30 | 0.58 | 0.39 | 0.78 | - |
| $f_3{}^a$ (%) | 0.07 | - | 0.19 | - | 0.15 | 0.05 | 0.4 | 0.38 | 0.11 | - |

$^a$In MeOH. $^b$In DMSO. $^c$In 50 mM phosphate buffer pH 7.0. $^d$Second maxima observed at the red edge of the excitation spectra.

was mainly observed in alkaline phosphate buffer (Figure 3d). A more moderate change in the absorption spectra was observed in MeOH and DMSO (see SI) indicating a ground-state deprotonation of the pyrimidine triazole scaffold.

The click adduct **20** of the 2-azidoadenosine **19** and DBCO exhibited the highest fluorescence quantum yield (10.6%), the largest Stokes shift (133 nm), and was the brightest (1.74 M$^{-1}$ cm$^{-1}$) of the library of compounds that were prepared and tested. The 2-adenosine-OCT adduct **18** was the second brightest compound (0.38 M$^{-1}$ cm$^{-1}$) and exhibited the second largest extinction coefficient (Table 1).

The effect of solvent polarity was explored for derivatives **7, 8, 11, 13, 17, 18, 20, 23,** and **27** in DMSO and phosphate buffer pH 7.0. We observed a 10 and 17 nm bathochromic shift

for **11** and **20** upon increasing solvent polarity (from DMSO to phosphate buffer at pH 7.0). Adduct **23** showed a more complex spectra upon increase in solvent polarity, with peaks at 324 and 440 nm undergoing bathochromic shifts of 10 and 5 nm. This uncorrelated shift in emission likely arises from multiple glycosyl bond conformers of **23** (*syn* vs *anti*) which are known to exhibit different photophysical properties.[79,80] The amplitude of the fluorescence emission was increased in DMSO for the uracil analogues, when compared to the intensity in MeOH and phosphate buffer. On the other hand, the intensity of the adenine derivatives was enhanced in MeOH and quenched in phosphate buffer, with exception of analogues **7** and **13** which were enhanced in DMSO (Figure S1 in SI). The observed increase in fluorescence intensity in an aprotic solvent

(i.e., DMSO) for the uracil derivatives correlates with the observed ground-state deprotonation of the uracil triazole moiety. The solvent effect on **7** and **11** show distinct responses despite their similar scaffolds, indicating that removal of the hydroxyl group at the C2′ likely induces a change in electron delocalization. Furthermore, introduction of a triazole ring at either the C2 or C8 positions likely causes a significant change in conformation (*anti* vs *syn*) thus changing the solvent sensitivity of the fluorophore, as shown by the OCT adducts **7** and **18** and by the DBCO adducts **13** and **20**.

All triazole products showed a complex fluorescence decay lifetime, with at least a triple discrete model needed to obtain a satisfactory fit (Figure 3), except analogue **8** which showed a biphasic decay. A fast lifetime of 0.1 to 0.6 ns was present in all compounds (Table 1). This fast decay is likely due to the fluorescence decay of the heterocyclic bases. In addition, 0.8–2.3 ns and 4.1–7.8 ns lifetime was recovered for all compounds, with **26** showing the longest lifetime (7.8 ns). The fractional contribution of each lifetime also varied among all triazole products; however, **11** (19%), **20** (40%), and **23** (38%) showed the largest contribution of the long lifetime ($\tau_3$). The longest average lifetime was observed for **20** (2.8 ns), followed by **23** (2.7 ns), **26** (2.7 ns), and **11** (1.6 ns). The recovered average fluorescence lifetime of the most fluorescent compounds is comparable to the lifetimes of current fluorescent proteins widely used in fluorescence lifetime imaging (FLIM),[81] and the utility of these fluorescent nucleoside analogues as probes in FLIM for real time measuring of metabolic activity inside living cells is discussed below.

**Cytotoxicity Assay.** Taking advantage that the click reaction between nonfluorescent azido nucleosides and cyclooctynes yields triazole products with strong fluorescence without the necessity for additional modification for visualization, we have tested its application to in vivo studies and have demonstrated the viability of these reactions in living cells. A cell toxicity assay was used to determine the nontoxic dose of azides **2** or **21** and cyclooctyne **5** on the survival of MCF-7 cells cultured for a 24 h time period. Under these conditions, MCF-7 cells were subjected to the MTT assay that measured the ability of cells to reduce the methylthiazoletetrazolium dye. We measured activity of MCF-7 cells at the most active part of the cells' growth phase, which was at 50% cell confluency, 24 h after seeding. The *y*-axis of the dose−response graph represents cell viability correlated to metabolic activity. From the dose−response graph for the reaction between cyclooctyne **5** and either azide **2** or **21**, we determined that a 1 $\mu$M dosage of these reagents was noncytotoxic to MCF-7 cells for a 24 h exposure (Figure 4), and consequently, we utilized this dosage for subsequent fluorescent studies.
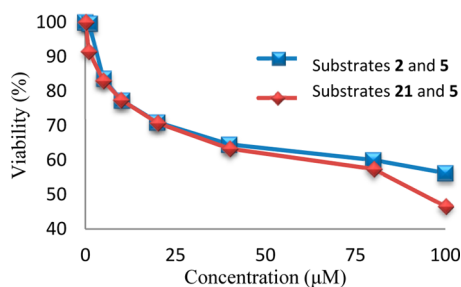


**Figure 4.** Cellular viability of MCF-7 cells when exposed to the click reactions between azides **2** or **21** and cyclooctyne **5**.

**Cellular Permeability.** A parallel artificial membrane permeation assay (PAMPA)[82] was used to predict cellular permeability of selected azides **2**, **4**, **19**, and **23** and triazole adducts **11** and **20**. A correlation between drug permeation across an alkane liquid membrane and percent absorption in humans has previously been shown; thus, a PAMPA assay provides an accurate model in depicting the passive absorption of the tested compounds across a cellular membrane.[83−86] The results showed that approximately 20% of each of the compounds tested passively permeated in through the cellular membrane and into the cells (Table 2). However, since

**Table 2. Cellular Permeability Data for the Selected Azides and Triazole Adduct**

| compound | % fraction absorbed | Log $P_e$ (cm/s)[a] |
|---|---|---|
| **2**[b] | 18 | −0.5 |
| **4** | 20 | −0.5 |
| **11** | 21 | −0.3 |
| **19** | 22 | −0.5 |
| **20** | 22 | −0.03 |
| **23** | 20 | −0.4 |

[a]Log of the effective permeability coefficient, $P_e$ (cm·s$^{-1}$), as assessed by a parallel artificial membrane permeability assay (HDM-PAMPA) performed at 75 $\mu$M concentrations. [b]Permeability for **2** at a 150 $\mu$M concentration was also 18%.

nucleoside transport proteins are also responsible for the cellular uptake of natural and modified nucleosides,[87] one can expect that the membrane proteins might also contribute to the overall uptake of these nucleoside-based theranostics.

**In Vivo Images.** The click chemistry between 8-azido-*arabino*-Ado **2** and cyclooctyne **5** was carried out in MCF-7 breast cancer cells. Thus, MCF-7 cells were incubated for 3 h at 37 °C with **2** (1 $\mu$M). The click reaction commenced via the addition of DMEM/F12 (1:1) 1× cell media containing cyclooctyne **5** (1 $\mu$M). We observed strong blue fluorescence in live cells using excitation and absorbance filters 360/40 and 470/40 nm, respectively (Figure 5), which was comparable to
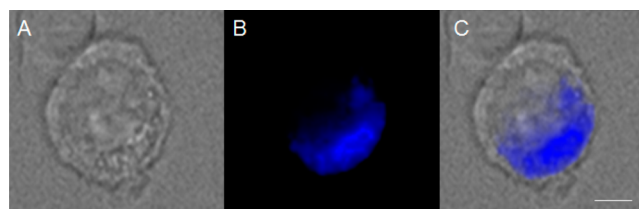


**Figure 5.** Fluorescence microscopy images and phase photos of live cells: (A) Phase photo of MCF-7 cells after the reaction of azide **2** with cyclooctyne **5**. (B) Fluorescent photo of the same MCF-7 cell. (C) Merged photo of panels (A) and (B). Scale = 20 $\mu$m.

the fluorescence that Ito et al. observed during the reaction of 8-azido-cAMP and a difluorinated cyclooctyne in HeLa cells.[46] However, contrary to this report, we found that the use of transfection agents (e.g., Lipofectamine; see SI for discussion), which often results in cytosol fluorescence, undue stress, and morphological changes in cells, was unnecessary.

In our negative controls, background fluorescence was indistinguishable in cells incubated without azide **2** or cyclooctyne **5**. Using a trypan blue fluorescence quenching mechanism,[88] we also concluded that fluorescence was intracellular and not due to the click reaction occurring on

the surface of the cell membrane. As shown in Figure 5, the 1 μM dose of compounds **2** and **5** showed a strong fluorescent localization to the nucleus. Similarly, in Figures 6 and 7, the 1 μM dose of azides **19** or **21** and **5** also showed fluorescence localized in the nucleus.
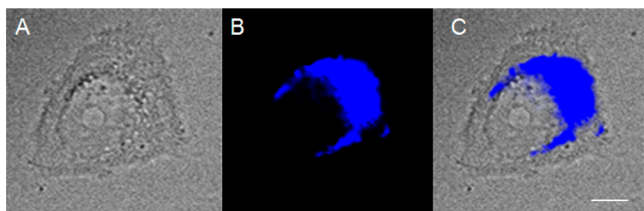


**Figure 6.** Fluorescence microscopy images and phase photos of live cells: (A) Phase photo of MCF-7 cells after the reaction of azide **19** with cyclooctyne **12**. (B) Fluorescent photo of the same MCF-7 cell. (C) Merged photo of panels (A) and (B). Scale = 20 μm.
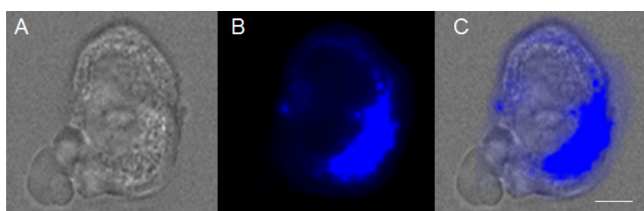


**Figure 7.** Fluorescence microscopy images and phase photos of live cells: (A) Phase photo of MCF-7 cells after the reaction azide **21** with cyclooctyne **5**. (B) Fluorescent photo of the same MCF-7 cell. (C) Merged photo of panels (A) and (B). Scale = 20 μm.

**Fluorescence Lifetime Imaging Microscopy.** In order to determine fluorescence lifetime within living cells, frequency-domain fluorescence lifetime imaging microscopy (FD-FLIM) was conducted on MCF-7 cells incubated with the triazole products **8**, **20**, or **23**. FD-FLIM is an imaging technique capable of image acquisition rates that are compatible with in vivo imaging, while also offering a means to visualize the individual lifetime components of a sample (i.e., the polar plot histogram).[89] This technique allows one to compare the lifetime characteristics, $\tau$ value, of compounds in vitro and in vivo.

After incubation of MCF-7 cells with triazoles **8**, **20**, or **23**, the fluorescent signals from cell nuclei were isolated for lifetime measurement and the average lifetimes from multiple cells were calculated for each compound (Table 3, Figure 8). The lifetime value obtained for *arabino* triazole adduct **8** was much higher in vivo (2.66 ns) than that found in vitro (1.60 ns; Table 1). This discrepancy in lifetimes suggests that in a methanol solution **8** can exist in two conformations (*syn* and *anti*) which populates the fast lifetime (0.6 ns). We also found that the mean lifetime

**Table 3. Mean Lifetime of Nucleoside Triazole Adducts within MCF-7 Cells as Determined by Frequency-Domain Lifetime Imaging (FD-FLIM)**

| compound | mean lifetime (ns) | SD | $n$ (# nuclei) | SEM |
|---|---|---|---|---|
| **8** | 2.66 | 0.159 | 13 | 0.044 |
| **8**[a] | 2.61 | 0.103 | 11 | 0.031 |
| **20** | 2.66 | 0.102 | 16 | 0.026 |
| **23** | 2.73 | 0.093 | 14 | 0.025 |

[a]Triazole adduct **8** synthesized by in vivo click reaction.

of triazole **8** was not altered when **8** had been synthesized by an in vivo click reaction between azide **2** and cyclooctynes **5** in MCF-7 cells (Table 3, footnote *a*).

The values for click adducts **20** (2.66 ns) and **23** (2.73 ns) were similar to those obtained through spectroscopic methods (see Table 1), although slightly lower. Polar plot analysis reveals that adduct **20** maintains its individual lifetime components (Figure 8), suggesting that the conformation found in vitro is also present in vivo. We believe that this can be attributed to steric hindrance and the size of the bulky DBCO component. The histogram for adduct **23** indicates that its lifetime components undergo an alteration in vivo; however, it still possesses more than one lifetime component, evidenced by its polar plot coordinates not falling exactly on the semicircle (Figure 8). As shown in Figure 3d and in the SI data, this compound is the most sensitive of all the compounds tested to pH and solvent polarity; thus, it is not entirely surprising to see differences between fluorescence lifetimes in vitro and within living cells. In addition to featuring a different solvent, the intranuclear environment may introduce a higher pH[90] or π-orbital stacking when compounds are DNA-bound, both of which can alter the fluorescence lifetime characteristics of a given compound.[91,92]

Although the lifetime properties of **8** and **23** change slightly within cells compared to in vitro determination, we found that their intracellular lifetimes are also relatively consistent from cell to cell and thus prove unambiguously the presence of **8**, **20**, and **23** within the nucleus. Therefore, all three compounds can serve as viable fluorescent probes in vivo, with adduct **20** being the compound of choice when low environmental sensitivity (i.e., lifetime invariance) is desired.

The present in situ click chemistry drug delivery system represents a novel approach wherein both a therapeutic effect and drug uptake-related imaging information may be produced and readily monitored at the cellular level. Although it is beyond the scope of this paper, the long-term implications of this in situ click chemistry drug delivery strategy embodied in click substrates (e.g., **2**, **19**, and **21**) could allow for a more precise monitoring of dosage levels, as well as an improved understanding of cellular uptake. It is also noteworthy that our nucleobase-derived triazole adducts can be visualized using fluorescent microscopy and FLIM without reliance on auxiliary fluorescent reporters such as green-fluorescent proteins[93] or Alexa Fluor.[14]

## ■ CONCLUSIONS

We have developed an efficient strain-promoted click chemistry between 2- or 8-azidoadenine and 5-azidouracil nucleosides as well as 8-azidoadenosine triphosphate with various cyclooctynes to produce highly functionalized triazole products. The reactions occur in cell culture media or aqueous organic solution at ambient temperature without the assistance of copper and/or microwave heating. We discovered that 5-azidouridine substrates were significantly more reactive than the 2- or 8-azidoadenosine precursors, whereas the position of the azido group on the adenine scaffold did not affect reactivity of adenosine substrates. We found that the novel triazole products have sufficient fluorescent properties which were used for direct imaging in living MCF-7 cancer cells without the need of any extra fluorophores. Using fluorescence lifetime imaging (FLIM) of living cancer cells, we have demonstrated, for the first time, the potential utility of triazole modified nucleobases for
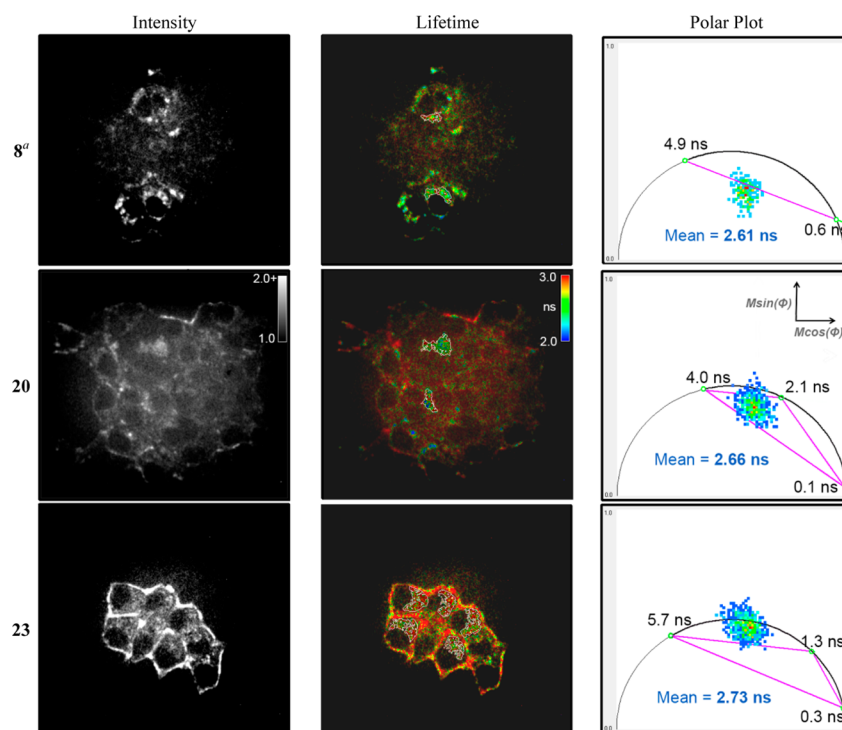
**Figure 8.** Representative images of fluorescence intensity (left column), fluorescence lifetime (middle column), and Polar Plot histogram (right column) for triazole adducts **8**, **20**, and **23** (1 $\mu$M) within MCF-7 cells. Fluorescence intensity images display an intensity range from 1.0 (background intensity) to 2.0+ (2× background and greater). Fluorescence lifetime heat maps display lifetimes ranging from 2.0 ns (and below) in blue to 3.0 ns (and above) in red. Polar plot histograms depict the $x,y$ coordinates [$M \cos(\Phi_F)$, $M \sin(\Phi_F)$] of pixels with intensities ranging from 1 (and below) in blue to 100 (and above) in red within nuclei (outlined in the corresponding lifetime image). Experimental component lifetimes are indicated on the semicircle (green circles), as well as the group mean lifetime for the specific compound. (*a*) Images for **8** are for the triazole adduct synthesized using an in vivo click reaction.

dynamic measuring and tracking of signaling events inside single living cells.

## EXPERIMENTAL PROCEDURES

**Materials and General Methods.** Detailed methods and characterization can be found in the Supporting Information. The $^1$H (400 MHz), $^{19}$F NMR (376.4 MHz), and $^{13}$C (100.6 MHz) were recorded at ambient temperature in solutions of ACN-$d_3$, D$_2$O, or DMSO-$d_6$, as noted. The reactions were followed by TLC with Merck Kieselgel 60-F254 sheets, and products were detected with a 254 nm light. Column chromatography was performed using Merck Kieselgel 60 (230−400 mesh). Reagent-grade chemicals were used. Azido nucleoside substrates were prepared as described in literature (**1**,[59] **2**,[61] **4**,[62] and **22**[70]) or in SI section (**3**), or are commercially available (**19**, **21**, and **28**) from Carbosynth. Cyclooctynes **5**, **6**, **12**, and **16** are commercially available from Kerafast, SynAffix, Sigma-Aldrich, or Berry & Associates. Lipofectamine LTX and Plus reagent was purchased from Invitrogen. HPLC analysis was performed on a semipreparative Phenomenex Gemini RP-C18 column (5 $\mu$, 25 cm × 1 cm) with UV detection at 254 nm.

**Synthetic Procedures.** *8-(1,2,3-Triazol-1H-yl)adenosine-OCT adduct (7). Typical Procedure.* Cyclooctyne **5** (*endo*; 7.6 mg, 0.05 mmol) was added to a stirred solution of 8-azidoadenosine[59] **1** (15.0 mg, 0.05 mmol) in a mixture of ACN/H$_2$O (3:1, 1 mL) at ambient temperature. After 3 h, the volatiles were evaporated in vacuo and the resulting residue was purified on silica gel column chromatography (20% MeOH/EtOAc) to give **7** as mixture of regioisomers (1:1; 21.0 mg,

96%) as a white solid. Alternatively the crude reaction mixture was passed through a 0.2 $\mu$m PTFE syringe filter, and then purified on the semipreparative HPLC column (17% ACN/H$_2$O, 2.0 mL/min) to give **7** (1:1; 21.0 mg, 96%) as a white solid ($t_R$ = 4.5−8.2 min): UV $\lambda_{max}$ 270 nm ($\varepsilon$ 21 100), $\lambda_{min}$ 241 nm ($\varepsilon$ 12 100); $^1$H NMR (DMSO-$d_6$) $\delta$ 0.84−0.95 (m, 2H, H$\gamma$), 0.99 ("q", $J$ = 9.4 Hz, 0.5H, CH cyclopropyl), 1.00 (q, $J$ = 9.4 Hz, 0.5H, CH cyclopropyl), 1.51−1.74 (m, 2H, H$\beta$), 2.00−2.19 (m, 2H, H$\beta$), 2.57−2.67 (m, 1H, H$\alpha$), 2.77−2.87 (m, 1H, H$\alpha$), 2.87−2.99 (m, 1H, H$\alpha$), 3.09−3.15 (m, 1H, H$\alpha$), 3.42−3.53 (m, 3H, CH$_2$ and H5′), 3.58 ("dq" $J$ = 12.2, 4.2 Hz, 1H, H5″), 3.85−3.93 (m, 1H, H4′), 4.00−4.07 (m, 1H, H3′), 4.35 (t, $J$ = 4.9 Hz, 1H, OH), 4.93 ("q", $J$ = 5.2 Hz, 0.5H, H2′), 5.00 ("q", $J$ = 5.2 Hz, 0.5H, H2′), 5.12−5.23 (m, 2H, H1′ and OH), 5.36−5.52 (m, 2H, 2 × OH), 7.78 (br s, 2H, NH$_2$), 8.23 (s, 1H, H2); $^{13}$C NMR (CD$_3$CN) $\delta$ 18.44, 18.58, 18.62, 20.14, 20.22, 20.82, 20.88, 21.21, 21.30, 22.33, 22.44, 25.04, 58.02, 58.81, 62.08, 69.18, 70.83, 71.01, 72.39, 72.44, 72.56, 86.96, 87.05, 89.39, 90.92, 138.39, 138.42, 138.47, 144.87, 144.93, 148.52, 152.01, 153.35, 156.31; HRMS (ESI$^+$) $m/z$ calcd C$_{20}$H$_{27}$N$_9$O$_5$ (M+H)$^+$: 459.2054, found: 459.2050.

Note: Analogous treatment of **1** (7.0 mg, 0.023 mmol) with **5** (4.7:1, *exo:endo*; 3.4 mg, 0.023 mmol) also gave **7** (~1:1; 10.0 mg, 96%).

*9-($\beta$-D-Arabinofuranosyl)-8-(1,2,3-triazol-1H-yl)adenine-OCT adduct (8).* Cyclooctyne **5** (4.7:1, *exo:endo*; 4.9 mg, 0.02 mmol) was added to a stirred solution of **2**[61] (10.0 mg, 0.02 mmol) in a mixture of ACN/H$_2$O (3:1, 1 mL) at ambient temperature. After 1 h, the volatiles were evaporated in vacuo and the resulting residue was purified by column chromatog-

raphy on silica gel (EtOAc → 20% MeOH/EtOAc) to give **8** as mixture of regioisomers (∼1:1; 12.8 mg, 93%) as a white solid: UV $\lambda_{max}$ 273 nm ($\varepsilon$ 17 500), $\lambda_{min}$ 248 nm ($\varepsilon$ 8700); ^{1}H NMR (DMSO-$d_6$) $\delta$ 0.83−0.96 (m, 2H, 2 × H$\gamma$), 0.96−1.07 (m, 1H, CH cyclopropyl), 1.50−1.70 (m, 2H, 2 × H$\beta$), 2.01−2.19 (m, 2H, 2 × H$\beta$), 2.56−2.71 (m, 1H, H$\alpha$), 2.78−2.95 (m, 2H, 2 × H$\alpha$), 3.11 ("q", $J$ = 3.3 Hz, 0.5H, H$\alpha$), 3.15 ("q", $J$ = 3.6 Hz, 0.5H, H$\alpha$), 3.46−3.53 (m, 1H, H5′), 3.58−3.66 (m, 3H, H5″ and $CH_2OH$), 4.20 (q, 1H, $J$ = 5.6 Hz, H4′), 4.26−4.37 (m, 1H, H2′ and H3′), 5.08−5.15 (m, 1H, OH), 5.41 (br s, 1H, OH), 5.63−5.67 (m, 1H, OH), 5.69 (d, $J$ = 6.7 Hz, 0.5H, H1′), 5.71 (d, $J$ = 6.8 Hz, 0.5, H1′), 7.61 (s, 2H, NH$_2$), 8.23 (s, 1H, H2); ^{13}C NMR (DMSO-$d_6$) $\delta$ 13.34, 17.42, 17.49, 19.31, 19.84, 19.87, 20.36, 20.38, 21.65, 24.12, 24.17, 30.09, 35.23, 56.57, 59.73, 73.17, 73.28, 75.17, 75.24, 81.61, 81.69, 84.24, 84.27, 115.79, 137.15, 137.18, 137.42, 137.43, 143.29, 143.34, 148.43, 152.46, 154.95, 162.35; HRMS (ESI$^+$) $m/z$ calcd $C_{20}H_{26}N_8NaO_5$ (M+Na)$^+$: 481.1918, found: 481.1927.

*9-(β-D-Arabinofuranosyl)-8-(1,2,3-triazol-1H-yl)adenine-OCT-biotin adduct (9).* Cyclooctyne **6** (*endo*; 5.5 mg, 0.01 mmol) was added to a stirred solution of **2** (3.1 mg, 0.01 mmol) in a mixture of ACN/H$_2$O (3:1, 1 mL) at ambient temperature. After 2 h (TLC showed complete conversion to the more polar product), the volatiles were evaporated in vacuo and the resulting residue was purified by HPLC (as described for **7**) to give **9** (5.4 mg, 71%) as a white oil: HRMS (ESI$^+$) $m/z$ calcd $C_{20}H_{26}N_8NaO_5$ (M+Na)$^+$: 481.1918, found: 481.1927.

*9-(2-Deoxy-2-fluoro-β-D-arabinofuranosyl)-8-(1,2,3-triazol-1H-yl)adenine-OCT adduct (10).* Cyclooctyne **5** (*exo:endo*, 4.7:1; 3.7 mg, 0.025 mmol) was added to a stirred solution of **3** (7.6 mg, 0.025 mmol) in a mixture of ACN/H$_2$O (3:1, 1 mL) at ambient temperature. After 3 h (TLC and NMR showed complete conversion of **3** to **10**) the volatiles were evaporated in vacuo to give **10** as mixture of regioisomers (∼1:1; 11 mg, 98%) as a white solid: ^{1}H NMR (DMSO-$d_6$) $\delta$ 0.84−0.97 (m, 2H, 2 × H$\gamma$), 0.98−1.07 (m, 1H, CH cyclopropyl), 1.52−1.71 (m, 2H, 2 × H$\beta$), 2.00−2.19 (m, 2H, 2 × H$\beta$), 2.56−2.72 (m, 1H, H$\alpha$), 2.73−2.95 (m, 2H, 2 × H$\alpha$), 3.09−3.16 (m, 1H, H$\alpha$), 3.46−3.53 (m, 2H, $CH_2OH$), 3.54−3.67 (m, 2H, H5′ and H5″), 3.69−3.75 (m, 1H, OH), 4.31−4.38 (m, 1H, OH), 4.63−4.77 (m, 1H, H4′), 5.06−5.12 (m, 1H, H3′), 5.23 (dt, $J$ = 53.9, 5.7 Hz, H2′), 5.86−5.95 (m, 2H, H1′ and OH), 7.00 (br s, 2H, NH$_2$), 8.27 (s, 0.5H, H2), 8.28 (s, 0.5H, H2); ^{19}F NMR (DMSO-$d_6$) $\delta$ −198.52 (ddd, $J$ = 53.9, 21.4, 8.2 Hz, 0.5F), −199.01 (ddd, $J$ = 53.9, 21.5, 7.3 Hz, 0.5F); HRMS (ESI$^+$) $m/z$ calcd $C_{20}H_{26}FN_8O_4$ (M+H)$^+$: 461.2056, found: 461.2059.

*2′-Deoxy-8-(1,2,3-triazol-1H-yl)adenosine-OCT adduct (11).* Cyclooctyne **5** (*endo*; 15.7 mg, 0.1 mmol) was added to a stirred solution of **4**[62] (29.5 mg, 0.1 mmol) in a mixture of ACN/H$_2$O (3:1, 1 mL) at ambient temperature. After 3 h, the crude reaction mixture was passed through a 0.2 $\mu$m PTFE syringe filter, and then purified on the semipreparative HPLC column (17% ACN/H$_2$O, 2.0 mL/min) to give **11** as mixture of regioisomers (1:1; 49.3 mg, 96%) as a white solid ($t_R$ = 13.0−16.2 min): UV $\lambda_{max}$ 272 nm ($\varepsilon$ 18 200), $\lambda_{min}$ 238 nm ($\varepsilon$ 8500); ^{1}H NMR (DMSO-$d_6$) 0.82−0.95 (m, 2H, 2 × H$\gamma$), 0.96−1.07 (m, 1H, CH cyclopropyl), 1.53−1.72 (m, 2H, 2 × H$\beta$), 2.03−2.19 (m, 3H, H2′ and 2 × H$\beta$′), 2.60−2.72 (m, 2H, 2 × H$\alpha$), 2.81−2.97 (m, 2H, 2 × H$\alpha$), 3.03−3.18 (m, 3H, H2″ and 2 × H$\alpha$), 3.37−3.45 (m, 1H, H5′), 3.47−3.59 (m, 3H, H5′ and $CH_2OH$), 3.76−3.82 (m, 1H, H4′), 4.30−4.37 (m, 2H, H3′ and OH), 5.26 (d, $J$ = 4.0 Hz, 1H, OH), 5.27−5.34 (m, 1H, OH), 5.71 (dd, $J$ = 6.4, 3.1 Hz, 0.5H, H1′), 5.73 (dd, $J$ = 6.4,

3.2 Hz, 0.5H, H1′), 7.72 (br s, 2H, NH$_2$), 8.26 (s, 1H, H2); HRMS (ESI$^+$) $m/z$ calcd $C_{20}H_{27}N_8O_4$ (M+H)$^+$: 443.2150, found: 443.2142.

*8-(1,2,3-Triazol-1H-yl)adenosine-DBCO adduct (13).* Cyclooctyne **12** (15.0 mg, 0.055 mmol) was added to a stirred solution of **1** (16.4 mg, 0.055 mmol) in a mixture of ACN/H$_2$O (3:1, 1.5 mL) at 50 °C. After 16 h, the crude reaction mixture was passed through a 0.2 $\mu$m PTFE syringe filter, and then injected into a semipreparative HPLC column (40% ACN/H$_2$O 1.0 mL/min) to give **13** (10.6 mg, 98%) as a mixture of several inseparable regioisomers ($t_R$ = 15.5−23.0 min): UV $\lambda_{max}$ 276 nm ($\varepsilon$ 16 000), $\lambda_{sh}$ 307 nm ($\varepsilon$ 11 200), $\lambda_{min}$ 270 nm ($\varepsilon$ 14 500). Two major isomers (∼85−90% of total isomeric composition) had: ^{1}H NMR (DMSO-$d_6$) $\delta$ 1.64−1.78 (m, 2H, NH$_2$), 2.08−2.33 (m, 2H, $CH_2CO$), 2.67−2.81 (m, 2H, $CH_2NH_2$), 3.31−4.18 (m, 4H, H3′, H4′, H5′ and H5″), 4.59 ("dm", $J$ = 17.1 Hz, 1H, CH$_2$), 5.08−5.18 (m, 1H, H2′), 5.19−5.55 (m, 3H, 3 × OH), 5.72 (d, $J$ = 7.5 Hz, 0.5H, H1′), 5.83 (d, $J$ = 7.0 Hz, 0.5H, H1′), 5.96 (br d, $J$ = 17.6 Hz, 1H, CH$_2$), 6.09 (br d, $J$ = 17.4 Hz, 1H, CH$_2$), 7.26−7.56 (m, 8H, H$_{ar}$), 8.25 (s, 0.5H, H2), 8.28 (s, 0.5H, H$_2$); HRMS (ESI$^+$) $m/z$ calcd $C_{28}H_{29}N_{10}O_5$ (M+H)$^+$: 585.2317, found: 585.2330.

*9-(β-D-Arabinofuranosyl)-8-(1,2,3-triazol-1H-yl)adenine-DBCO adduct (14).* Cyclooctyne **12** (5.72 mg, 0.02 mmol) was added to a stirred solution of **2** (4.0 mg, 0.02 mmol) in MeOH (1 mL) at 50 °C. After 16 h, the crude reaction mixture was passed through a 0.2 $\mu$m PTFE syringe filter, and then injected into a semipreparative HPLC column (Phenomenex Gemini RP-C18 column; 5 $\mu$, 25 cm × 1 cm) (40% ACN/H$_2$O, 1.5 mL/min) to give **14** (8.52 mg, 95%) as a mixture of several inseparable regioisomers ($t_R$ = 5.5−10.0 min): ^{1}H NMR (DMSO-$d_6$) $\delta$ 2 major isomers (∼85−90% of total isomeric composition) had: ^{1}H NMR (DMSO-$d_6$) $\delta$ 1.42−1.78 (m, 2H, NH$_2$), 2.01−2.17 (m, 2H, $CH_2CO$), 2.60−2.78 (m, 2H, $CH_2NH_2$), 3.17−3.24 (m, 2H, H4′ and H5′), 3.28 (dd, $J$ = 11.5 Hz, 4.6 Hz, 1H, H5″), 3.83−3.87 (m, 1H, H3′), 4.10 (t, $J$ = 6.0 Hz, 0.5H, H2′), 4.11 (t, $J$ = 5.9 Hz, 0.5H, H2′), 4.49 (br s, 2H, CH$_2$), 5.72 (d, $J$ = 5.1 Hz, 1H, H1′), 7.26−7.56 (m, 8H, H$_{ar}$), 8.09 (s, 1H, H2); HRMS (ESI$^+$) $m/z$ calcd $C_{28}H_{29}N_{10}O_5$ (M +H)$^+$: 585.2317, found: 585.2425.

*2′-Deoxy-8-(1,2,3-triazol-1H-yl)adenosine-DBCO adduct (15).* Cyclooctyne **12** (4.7 mg, 0.015 mmol) was added to a stirred solution of **4** (4.9 mg, 0.015 mmol) in MeOH (1.5 mL) at 50 °C. After 16 h, the crude reaction mixture was passed through a 0.2 $\mu$m PTFE syringe filter, and then injected into a semipreparative HPLC column (Phenomenex Gemini RP-C18 column; 5 $\mu$, 25 cm × 1 cm (40% ACN/H$_2$O, 2.0 mL/min) to give **15** (9.5 mg, 95%) as a mixture of several inseparable regioisomers ($t_R$ = 8.5−5.0 min): UV $\lambda_{max}$ 273 nm ($\varepsilon$ 12 550); ^{1}H NMR (DMSO-$d_6$) $\delta$ 1.64−1.81 (m, 2H, NH$_2$), 2.11−2.15 (m, 1H, H2′), 2.15−2.30 (m, 2H, $CH_2CO$), 2.60−2.79 (m, 2H, $CH_2NH_2$), 3.34−3.95 (m, 4H, H3′, H4′, H5′ and H5″), 4.51− 4.60 (m, 2H, CH$_2$), 4.91 (dd, $J$ = 5.8, 2.3 Hz, 1H, H2′), 5.18− 5.48 (m, 3H, 3 × OH), 5.74 (d, $J$ = 6.7 Hz, 0.5H, H1′), 5.76 (d, $J$ = 6.2 Hz, 0.5H, H1′), 5.94 (br d, $J$ = 15.8 Hz, 1H, CH$_2$), 6.12 (br d, $J$ = 16.4 Hz, 1H, CH$_2$), (6.86−7.84 (m, 8H, H$_{ar}$), 8.4 (s, 0.5H, H2), 7.94 (s, 0.5H, H2); HRMS (ESI$^+$) $m/z$ calcd $C_{28}H_{29}N_{10}O_4$ (M+H)$^+$: 569.2368, found: 569.2411.

*8-(1,2,3-Triazol-1H-yl)adenosine-MFCO Adduct (17).* Cyclooctyne **16** (6.25 mg, 0.02 mmol) was added to a stirred solution of **1** (6.25 mg, 0.02 mmol) in MeOH (1 mL) at ambient temperature. After 16 h, the volatiles were evaporated in vacuo to give cycloadduct **17** (1:1; 12.3 mg, 98%) as a clear

oil: UV $\lambda_{max}$ 271 nm ($\varepsilon$ 16 400), $\lambda_{min}$ 242 nm ($\varepsilon$ 8000); $^1$H NMR (DMSO-$d_6$/D$_2$O) $\delta$ 1.43–1.50 (m, 6H, 3 × CH$_2$), 1.56–1.67 (m, 4H, 2 × CH$_2$), 1.67–1.75 (m, 2H, CH$_2$), 2.23–2.34 (m, 2H, CH$_2$), 2.54–2.60 (m, 2H, CH$_2$), 2.60–2.67 (m, 2H, CH$_2$), 2.76–2.82 (br s, 4H, 2 × CH$_2$), 3.04–3.13 (m, 2H, CH$_2$), 3.45 ("dd", $J$ = 10.8, 2.3 Hz, 1H, H5′), 3.51 ("dd", $J$ = 2.2 Hz, 10.9 Hz, 1H, H5″), 3.87–3.90 (m, 0.5H, H4′), 3.91–3.95 (m, 0.5H, H4′), 4.03 (m, 0.5H, H3′), 4.09 (m, 0.5H, H3′), 4.97 (t, $J$ = 4.9 Hz, 0.5H, H2′), 4.98 (t, $J$ = 5.1 Hz, 0.5H, H2′), 5.27 (d, $J$ = 7.0 Hz, 0.5 H, H1′), 5.28 (d, $J$ = 7.1 Hz, 0.5 H, H1′), 8.27 (s, 0.5H, H2), 8.28 (s, 0.5H, H2); HRMS (ESI$^+$) $m/z$ calcd C$_{29}$H$_{37}$FN$_{10}$NaO$_9$ (M+Na)$^+$: 711.2621, found: 711.2543.

*2-(1,2,3-Triazol-1H-yl)adenosine-OCT adduct (18).* Cyclo-octyne **5** (4.7:1 *exo:endo* mixture; 3.13 mg, 0.020 mmol) was added to a stirred solution of 2-azidoadenosine$^{94}$ **19** (6.25 mg, 0.020 mmol) in a mixture of ACN/H$_2$O (3:1, 1 mL) at ambient temperature. After 2 h, the volatiles were evaporated in vacuo to give **18** (9.3 mg, 100%) as a white solid: UV $\lambda_{max}$ 261 nm ($\varepsilon$ 19 100), $\lambda_{min}$ 246 nm ($\varepsilon$ 16 600); $^1$H NMR (DMSO-$d_6$) $\delta$ 0.81–0.89 (m, 2H, 2 × H$\gamma$), 0.94–1.04 (m, 1H, CH cyclopropyl), 1.56–1.72 (m, 2H, 2 × H$\beta$), 2.06–2.22 (m, 2 H, 2 × H$\beta$), 2.81–2.90 (m, 1H, H$\alpha$), 2.99–3.14 (m, 2H, 2 × H$\alpha$), 3.15–3.19 (m, 1H, H$\alpha$), 3.44–3.58 (m, 3H, H5′ and CH$_2$), 3.59–3.69 (m, 1H, H5″), 4.11–4.16 (m, 1H, H4′), 4.35 (t, $J$ = 5.0 Hz, 1H, H3′), 4.59 ("quint", $J$ = 6.0 Hz, 1H, H2′), 4.99–5.04 (m, 1H, OH), 5.21 (d, $J$ = 4.9 Hz, 1H, OH), 5.45–5.53 (m, 2H, 2 × OH), 5.89 (d, $J$ = 5.8 Hz, 1H, H1′), 7.89 (br s, 2H, NH$_2$), 8.52 (s, 1H, H8); HRMS (ESI$^+$) $m/z$ calcd C$_{20}$H$_{27}$N$_9$O$_5$ (M+H)$^+$: 459.2099, found: 459.2098.

*2-(1,2,3-Triazol-1H-yl)adenosine-DBCO Adduct (20).* Cyclooctyne **12** (9.67 mg, 0.035 mmol) was added to a stirred solution of **19** (10.93 mg, 0.035 mmol) in MeOH (1 mL) at ambient temperature. After 16 h, the volatiles were evaporated in vacuo and the residue was passed through a 0.2 $\mu$m PTFE syringe filter, and then purified on the semipreparative HPLC column (17% ACN/H$_2$O, 2.0 mL/min) to give **20** (17.5 mg, 85%) as a mixture of several inseparable isomers ($t_R$ = 13.0–16.2 min): UV $\lambda_{max}$ 263 nm ($\varepsilon$ 16 400), $\lambda_{sh}$ 274 nm ($\varepsilon$ 9600), $\lambda_{min}$ 253 nm ($\varepsilon$ 15 200); 2 major isomers (~85–90% of total isomeric composition) had: $^1$H NMR (DMSO-$d_6$) $\delta$ 1.58–1.62 (m, 2H, NH$_2$), 2.03–2.09 (m, 2H, CH$_2$CO), 2.57–2.72 (m, 2H, CH$_2$NH$_2$), 3.49–3.50 (m, 1H, H5′), 3.69 (dd, $J$ = 11.8 Hz and 3.3 Hz, 1H, H5″), 3.83–3.94 (m, 1H, H4′), 4.07–4.16 (m, 1H, H3′), 4.38 (t, $J$ = 5.1 Hz, 0.5H, H2′), 4.44 (t, $J$ = 5.0 Hz, 0.5H, H2′), 4.53 ("dm", $J$ = 17.0 Hz, 1H, CH$_2$), 4.86–5.47 (m, 3H, 3 × OH), 5.67 (d, $J$ = 7.1 Hz, 0.5H, H1′), 5.82 (d, $J$ = 7.2 Hz, 0.5H, H1′), 5.96 (br d, $J$ = 19.7 Hz, 2H, CH$_2$), 7.06–7.52 (m, 8H, H$_{ar}$), 8.54 (s, 0.5H, H8), 8.55 (s, 0.5H, H8); HRMS (ESI$^+$) $m/z$ calcd C$_{28}$H$_{29}$N$_{10}$O$_5$ (M+H)$^+$: 585.2317, found: 585.2318.

*5-(1,2,3-Triazol-1H-yl)uridine-OCT Adduct (23).* Cyclooctyne **5** (4.0 mg, 0.025 mmol) was added to a stirred solution of 5-azidouridine **21** (7.3 mg, 0.025 mmol) in a mixture of ACN/H$_2$O (3:1, 1 mL) at ambient temperature. After 15 min, the volatiles were evaporated in vacuo, and the oily residue was passed through a 0.2 $\mu$m PTFE syringe filter, and then purified on the semipreparative HPLC column (20% ACN/H$_2$O, 2.0 mL/min; $t_R$ = 5.2–8.0 min) to give **23** (6.2 mg, 77%) as a 1:1 mixture of isomers: UV $\lambda_{max}$ 270 nm ($\varepsilon$ 10 100) $\lambda_{min}$ 248 nm ($\varepsilon$ 6800); $^1$H NMR (DMSO-$d_6$) $\delta$ 0.85–0.93 (m, 2H, 2 × H$\gamma$), 0.95–1.02 (m, 1H, CH cyclopropyl), 1.46–1.56 (m, 2H, 2 × H$\beta$), 1.99–2.14 (m, 2H, 2 × H$\beta$), 2.72–2.83 (m, 2H, 2 × H$\alpha$), 3.00–3.04 (m, 0.5H, H$\alpha$), 3.05–3.08 (m, 0.5H, H$\alpha$), 3.16–

3.18 (d, $J$ = 5.2 Hz, 1H, H$\alpha$), 3.50 (dd, $J$ = 2.5, 12.0 Hz, 1H, H5′), 3.59–3.62 (m, 1H, H5″), 3.85–3.89 (m, 1H, H4′), 3.95–4.01 (m, 1H, H3′), 4.10 ("q", $J$ = 4.6 Hz, 1H, H2′), 4.36 (t, $J$ = 4.9 Hz, 1H, OH), 5.09–5.14 (m, 2H, 2 × OH), 5.51–5.55 (m, 1H, OH), 5.78 (d, $J$ = 4.0 Hz, 0.5H, H1′), 5.79 (d, $J$ = 3.9 Hz, 0.5H, H1′), 8.52 (s, 0.5H, H2), 8.53 (s, 0.5H, H2); HRMS (ESI$^+$) $m/z$ calcd C$_{19}$H$_{27}$N$_5$O$_7$ (M+H)$^+$: 436.1827, found: 436.1829.

*5-(1,2,3-Triazol-1H-yl)uridine-biotin Adduct (24).* Cyclooctyne **6** (11.0 mg, 0.02 mmol) was added to a stirred solution of 5-azidouridine **21** (5.6 mg, 0.02 mmol) in a mixture of ACN/H$_2$O (3:1, 1 mL) at ambient temperature. After 3 min, the volatiles were evaporated in vacuo to give cycloadduct **24** (16.0 mg, 98%) as a white solid: HRMS (ESI$^+$) $m/z$ calcd C$_{36}$H$_{53}$N$_9$O$_{12}$S (M+H)$^+$: 836.3607, found: 836.3562.

*2′-Deoxy-8-(1,2,3-triazol-1H-yl)uridine-OCT Adduct (25).* Cyclooctyne **5** (4.7:1 *exo:endo* mixture; 14.3 mg, 0.1 mmol) was added to a stirred solution of **22**$^{70}$ (26.7 mg, 0.1 mmol) in a mixture of ACN/H$_2$O/MeOH (3:1:1, 1 mL) at ambient temperature. After 15 min, the volatiles were evaporated in vacuo to give cycloadduct **25** as mixture of isomers (~1:1; 15.3 mg, 100%) as a white solid: $^1$H NMR (DMSO-$d_6$) $\delta$ 0.83–0.94 (m, 2H, 2 × H$\gamma$), 0.95–1.05 (m, 1H, CH cyclopropyl), 1.42–1.59 (m, 2H, 2 × H$\beta$), 1.98–2.14 (m, 2H, 2 × H$\beta$), 2.20 ("t", $J$ = 5.2 Hz, 2H, H2′ and H2″), 2.46–2.56 (m, 1H, H$\alpha$), 2.70–2.83 (m, 2H, 2 × H$\alpha$), 3.00–3.05 (m, 0.5H, H$\alpha$), 3.05–3.09 (m, 0.5H, H$\alpha$), 3.44–3.54 (m, 3H, H5′ and CH$_2$), 3.54–3.61 (m, 1H, H5″), 3.80 (q, $J$ = 3.2 Hz, 1H, H4′), 4.17–4.26 (m, 1H, H3′), 4.34 (m, 1H, OH), 5.02 (m, 1H, OH), 5.28 (m, 1H, OH), 6.15 (t, $J$ = 6.3 Hz, 0.5H, H1′), 6.16 (t, $J$ = 6.3 Hz, 0.5H, H1′), 8.43 (s, 0.5H, H6), 8.44 (s, 0.5H, H6); HRMS (ESI$^+$) $m/z$ calcd C$_{19}$H$_{26}$N$_5$O$_6$ (M+H)$^+$: 420.1878, found: 420.1878.

*5-(1,2,3-Triazol-1H-yl)uridine-DBCO Adduct (26).* Cyclooctyne **12** (5.6 mg, 0.02 mmol) was added to a stirred solution of **21** (5.5 mg, 0.02 mmol) in MeOH (1 mL) at ambient temperature. After 15 min, the volatiles were evaporated in vacuo and the residue was passed through a 0.2 $\mu$m PTFE syringe filter, and then injected into a semipreparative HPLC column (40% ACN/H$_2$O, 1.0 mL/min; $t_R$ = 7.0–12.0 min) to give **26** as an inseparable mixture of isomers (5.1 mg, 77%): UV $\lambda_{max}$ 276 nm ($\varepsilon$ 7300), 291 nm ($\varepsilon$ 7100), $\lambda_{sh}$ 309 nm ($\varepsilon$ 5400), $\lambda_{min}$ 265 nm ($\varepsilon$ 6750), 283 nm ($\varepsilon$ 7000), 303 nm ($\varepsilon$ 5000); HRMS (ESI$^+$) $m/z$ calcd C$_{27}$H$_{28}$N$_9$O$_7$ (M+H)$^+$: 562.2045, found: 526.2040.

*5-(1,2,3-Triazol-1H-yl)uridine-MFCO Adduct (27).* Cyclooctyne **16** (7.6 mg, 0.02 mmol) was added to a stirred solution of 5-azidouridine **21** (5.6 mg, 0.02 mmol) in MeOH (1 mL) at ambient temperature. After 12 min, the volatiles were evaporated in vacuo to give complete conversion to cycloadduct **27** as mixture of regioisomers (1:1; 12.9 mg, 100%) as a white solid: UV $\lambda_{max}$ 269 nm ($\varepsilon$ 7100), $\lambda_{min}$ 244 nm ($\varepsilon$ 5000); $^1$H NMR (DMSO-$d_6$) $\delta$ 1.40–1.50 (m, 6H, 3 × CH$_2$), 1.73–1.81 (m, 2H, CH$_2$), 2.27–2.34 (m, 2H, CH$_2$), 1.57–1.67 (m, 6H, 3 × CH$_2$), 2.48–2.53 (m, 2H, CH$_2$), 2.62–2.69 (m, 2H, CH$_2$), 2.78–2.86 (s, 4H, 2 × CH$_2$), 3.01–3.13 (m, 2H, CH$_2$), 3.47–3.54 (m, 1H, H5′), 3.60–3.65 (m, 1H, H5″), 3.94–3.99 (m, 1H, H4′), 4.08–4.15 (m, 1H, H3′), 4.27–4.36 (m, 1H, H2′), 5.06–5.11 (m, 2H, OH (2′) and OH (3′)), 5.51 (t, $J$ = 6.7 Hz, 1H, OH (5′)), 5.78 (d, $J$ = 4.9 Hz, 0.5H, H1′), 5.79 (d, $J$ = 4.6 Hz, 0.5H, H1′), 8.57 (s, 1H, H6); HRMS (ESI$^+$) $m/z$ calcd C$_{28}$H$_{36}$FN$_7$O$_{11}$ (M+H)$^+$: 666.2530, found: 666.2518.

*8-(1,2,3-Triazol-1H-yl)adenosine-OCT Adduct Triphosphate (29).* Cyclooctyne **5** (5.6 mg, 0.01 mmol) was added

to a stirred solution of 8-azidoadenosine 5′-triphosphate tetralithium salt **28** (3.2 mg, 0.01 mmol) in a mixture of ACN/H$_2$O (3:1, 1 mL) at ambient temperature. After 2 h, the volatiles were evaporated in vacuo to give **29** (3.2 mg, 92%) as a 1:1 mixture of regioisomers: $^1$H NMR (ACN-$d_3$/D$_2$O) $\delta$ 0.80−0.88 (m, 2H, 2 × H$\gamma$), 0.95−1.06 (m, 1H, CH cyclopropyl), 1.46−1.6 (m, 2H, 2 × H$\beta$), 2.06−2.28 (m, 2H, 2 × H$\beta$), 2.62−2.74 (m, 1H, H$\alpha$), 2.82−3.00 (m, 2H, 2 × H$\alpha$), 3.11−3.21 (m, 1H, H$\alpha$), 3.56−3.64 (m, 4H, H5′, H5″ and CH$_2$), 4.17−4.32 (m, 2H, H3′ and H4′), 4.89 (t, $J$ = 5.8 Hz, 0.5H, H2′), 4.97 (t, $J$ = 5.7 Hz, 0.5H, H2′), 5.47 (d, $J$ = 5.6 Hz, 0.5H, H1′), 5.51 (d, $J$ = 5.5 Hz, 0.5H, H1′), 8.32 (s, 0.5H, H2), 8.33 (s, 0.5H, H2); HRMS (ESI$^-$) $m/z$ calcd C$_{20}$H$_{28}$N$_8$O$_{14}$P$_3$ (M+H)$^-$: 697.0943, found: 697.0962.

**Photophysical Characterization.** The fluorescent properties of the triazole products were determined using samples of varying concentration but whose absorbance at the excitation wavelength did not exceed 0.1 absorbance units. For determination of $\Phi_F$ the absorbance was kept below 0.06 and quinine sulfate in 100 mM sulfuric acid was used as reference standard ($\Phi_F$ = 0.55).[95] All samples were prepared in HPLC grade MeOH or DMSO and in freshly prepared 50 mM phosphate buffer, and placed in a 2 × 10 mm quartz cuvette at 18 °C. Absorption spectra were measured using a single beam UV−vis spectrophotometer. Steady-state excitation and emission spectra were measured on a PC1 spectrofluorometer with bandwidth and slit width for excitation/emission set at 2 nm. Frequency-domain fluorescence lifetime measurements were performed using a ChronosFD spectrofluorometer. Samples were excited with a frequency modulated 280 nm LED and emission was collected using a 305 nm long-pass filter (Andover); 2,5-diphenyloxazole (PPO) solubilized in ethanol was used as a lifetime reference ($\tau$ = 1.4 ns).[96] Modulation-phase data were fitted by a multiple-exponential decay model using GlobalsWE software and the residual and $\chi^2$ parameter was used as criterion for goodness of fit.

**MTT Assay.** MCF-7 cells were seeded in 96-well plates at a density of 1 × 10$^4$ cells/mL and treated with different concentrations of azides **2** or **21** and cyclooctyne **5** for 24 h at 37 °C in a 5% CO$_2$ incubator. Methylthiazoletetrazolium (MTT) solution (5 mg/mL) was added to the assay mixture and incubated for 4 h. The culture media was removed prior to addition of DMSO. The optical density of the solution was measured at 595 nm, using an absorbance microplate reader (Bio-Tek). Cells without the treatment of the compounds were used as the control. The cell viability percentage was calculated by the following formula: Cell viability percentage (%) = OD sample/OD control × 100%.

**Cellular Permeability Measurements.** Parallel artificial membrane permeability assay (PAMPA) was used to determine effective permeability coefficients P$_e$ (centimeters per second), in a 96-well microtiter filter plates, on polycarbonate filter of 0.45 $\mu$m pore size, 10 $\mu$m thickness (Millipore AG, Volketswil, Switzerland), according to the procedure of Wohnsland and Faller.[82]

Each well was coated with 15 $\mu$L of lecitin (1% or 4% in dodecane solution) for 5 min avoiding pipet tip contact with the membrane. Compounds **2**, **4**, **11**, **19**, **20**, and **23** were dissolved in 5% DMSO in PBS solution (75 $\mu$M) and were tested at least in triplicate. The solution of each compound (300 $\mu$L each) was added to each well of the donor plate. Aqueous buffer (PBS) (300 $\mu$L) was added to each well of the acceptor plate and then the donor plate was placed upon the

acceptor plate. The resulting chamber was incubated at ambient temperature for 16 h at ambient temperature under gentle shaking. After incubation, it was carefully disassembled and each well of the acceptor plate was analyzed using UV−vis for compound concentration. A solution of each compound at its theoretical equilibrium (i.e., the resulting concentration of the donor and acceptor phases were simply combined) was similarly analyzed. The effective permeability (Log P$_e$) was calculated from the equation as reported.[82]

**Cell Microscopy Studies.** *Fluorescent Microscopy. Typical Procedure.* The MCF-7 cells (5 × 10$^5$ cells/mL) were seeded in an eight chambered coverglass system (1.5 German borosilicate coverglass, Lab-Tek II) and incubated at 37 °C overnight in Dulbecco's modified Eagle's medium (DMEM/F12 (1:1) 1×, 1.5 mL) containing 5% fetal bovine serum (FBS). The 8-azido-9-($\beta$-D-arabinofuranosyl)adenine **2** in the reduced serum medium (1 $\mu$M) was added to the cells. After 4 h, the cells were washed three times with fresh PBS (pH 7.5) media to remove any azide from the exterior portions of the cells. The cyclooctyne reagent **5** in reduced serum medium (1 $\mu$M) was then added to the medium and the cells were incubated at 37 °C for 16 h. The cells were then washed three times with fresh PBS (pH 7.5) media to remove any click adduct from the exterior portions of the cells and observed with a DV ELITE-microscope (Fisher Scientific) using excitation and absorbance filters were 360/40 and 470/40 nm, respectively.

In the first negative control, the MCF-7 cells were just incubated with azide **2** without the cyclooctyne reagent added. In the second negative control, the MCF-7 cells were just incubated with cyclooctyne **5**. Also, in the positive control the cells were treated with click adduct **11** dissolved in culture media. We used 0.1% trypan blue in the culture media before imaging the cells in DV ELITE microscope.

Note: In parallel experiments Lipofectamine LTX was used as liposome carrier.

*Fluorescent Lifetime Imaging Microscopy (FLIM). Typical Procedure.* Synthetically prepared triazole adduct **8**, **20**, or **23** as well as in vivo generated **8** [0.5 mL of 1 $\mu$M solution in DMEM/F12 (1:1) 1× media] was added to MCF-7 cells (∼50% cell confluency) cultured on slides mounted with 1-tissue culture well. After 24 h, the cells were washed twice with fresh (DMEM/F12 (1:1) 1×, 0.5 mL). The cells were then imaged at ambient temperature in fresh DMEM/F12 (∼0.2 mL).

Ex vivo lifetime measurements were acquired using a custom-assembled frequency-domain upright FLIM system from Intelligent Imaging Innovations Inc. (3i). A continuous-wave excitation source (488 nm argon laser) was modulated by a Pockels cell electro-optic modulator, which was synchronized with a Lambert Instruments II18MD gated image intensifier and CoolSnap EZ camera. A Yokogawa CSU-X1 spinning disk provided confocal scanning for fast image acquisition. A Zeiss W Plan-Apochromat 63× (n.a. 1.0) water-immersion objective lens and a Semrock 520 emission filters with a Semrock Di10 T488/568 diochroic were also used.

Image intensification was maintained at 2800 units across all experiments. Exposure times were set to acquire enough signal to span approximately 75% of the CCD's dynamic range; however, this time was never extended to more than 40 s (as such samples typically have low signal-to-noise. System calibration was performed with the fluorescent dye, 1-hydroxypyrene-3,6,8-trisulfonate (HPTS), in solution (PBS at

pH 7.5) for a standard lifetime of 5.4 ns. We found HPTS to be a reliable standard and superior to fluorescein, owing to its greater stability over time and pH shifts.

## ■ ASSOCIATED CONTENT

**Ⓢ Supporting Information**

Synthetic procedure for the preparation and characterization of **3**, additional fluorescence, and cellular imaging data and kinetic data. The Supporting Information is available free of charge on the ACS Publications website at DOI: 10.1021/acs.bioconjchem.5b00300.

## ■ AUTHOR INFORMATION

**Corresponding Author**

*E-mail: wnuk@fiu.edu. Phone: 305-348-6195.

**Author Contributions**

The manuscript was written through contributions of all authors. Study concept and design (J.Z., S.F.W.), synthesis (J.Z., M.A.), fluorescent microscopy (J.K.D., Q.F.), photophysical characterization (W.G., J.M.), and FLIM studies (N.S., A.C.). All authors have given approval to the final version of the manuscript.

**Notes**

The authors declare no competing financial interest.

## ■ ACKNOWLEDGMENTS

## ■ ABBREVIATIONS

DBCO, dibenzylcyclooctyne; FD-FLIM, frequency domain fluorescence lifetime imaging; MFCO, monofluorocyclooctyne; MTT, 3-(4,5-dimethylthiazol-2-yl)-2,5-diphenyltetrazolium bromide; OCT, cyclopropyl cyclooctyne; ODNs, oligodeoxynucleotides; SPAAC, strain promoted click chemistry

## ■ REFERENCES

(1) Hein, C. D., Liu, X. M., and Wang, D. (2008) Click chemistry, a powerful tool for pharmaceutical sciences. *Pharm. Res. 25*, 2216−2230.

(2) Nwe, K., and Brechbiel, M. W. (2009) Growing applications of "click chemistry" for bioconjugation in contemporary biomedical research. *Cancer Biother. Radiopharm. 24*, 289−302.

(3) Yang, P. Y., Wang, M., He, C. Y., and Yao, S. Q. (2012) Proteomic profiling and potential cellular target identification of K11777, a clinical cysteine protease inhibitor, in Trypanosoma brucei. *Chem. Commun. 48*, 835−837.

(4) Agard, N. J., Prescher, J. A., and Bertozzi, C. R. (2004) A Strain-Promoted [3 + 2] Azide−Alkyne Cycloaddition for Covalent Modification of Biomolecules in Living Systems. *J. Am. Chem. Soc. 126*, 15046−15047.

(5) Baskin, J. M., Prescher, J. A., Laughlin, S. T., Agard, N. J., Chang, P. V., Miller, I. A., Lo, A., Codelli, J. A., and Bertozzi, C. R. (2007) Copper-free click chemistry for dynamic in vivo imaging. *Proc. Natl. Acad. Sci. U.S.A. 104*, 16793−16797.

(6) Codelli, J. A., Baskin, J. M., Agard, N. J., and Bertozzi, C. R. (2008) Second-Generation Difluorinated Cyclooctynes for Copper-Free Click Chemistry. *J. Am. Chem. Soc. 130*, 11486−11493.

(7) Laughlin, S. T., and Bertozzi, C. R. (2009) In Vivo Imaging of Caenorhabditis elegans Glycans. *ACS Chem. Biol. 4*, 1068−1072.

(8) Gordon, C. G., Mackey, J. L., Jewett, J. C., Sletten, E. M., Houk, K. N., and Bertozzi, C. R. (2012) Reactivity of Biarylazacyclooctynones in Copper-Free Click Chemistry. *J. Am. Chem. Soc. 134*, 9199−9208.

(9) Ning, X., Guo, J., Wolfert, M. A., and Boons, G.-J. (2008) Visualizing Metabolically Labeled Glycoconjugates of Living Cells by Copper-Free and Fast Huisgen Cycloadditions. *Angew. Chem., Int. Ed. 47*, 2253−2255.

(10) Dommerholt, J., Schmidt, S., Temming, R., Hendriks, L. J., Rutjes, F. P., van Hest, J. C., Lefeber, D. J., Friedl, P., and van Delft, F. L. (2010) Readily accessible bicyclononynes for bioorthogonal labeling and three-dimensional imaging of living cells. *Angew. Chem., Int. Ed. 49*, 9422−9425.

(11) Debets, M. F., van Berkel, S. S., Schoffelen, S., Rutjes, F. P. J. T., van Hest, J. C. M., and van Delft, F. L. (2010) Aza-dibenzocyclooctynes for fast and efficient enzyme PEGylation via copper-free (3 + 2) cycloaddition. *Chem. Commun. 46*, 97−99.

(12) Jawalekar, A. M., Malik, S., Verkade, J. M. M., Gibson, B., Barta, N. S., Hodges, J. C., Rowan, A., and van Delft, F. L. (2013) Oligonucleotide Tagging for Copper-Free Click Conjugation. *Molecules 18*, 7346−7363.

(13) Laughlin, S. T., Baskin, J. M., Amacher, S. L., and Bertozzi, C. R. (2008) In Vivo Imaging of Membrane-Associated Glycans in Developing Zebrafish. *Science 320*, 664−667.

(14) Belardi, B., de la Zerda, A., Spiciarich, D. R., Maund, S. L., Peehl, D. M., and Bertozzi, C. R. (2013) Imaging the Glycosylation State of Cell Surface Glycoproteins by Two-Photon Fluorescence Lifetime Imaging Microscopy. *Angew. Chem., Int. Ed. 52*, 14045−14049.

(15) Kore, A. R., and Charles, I. (2013) Click Chemistry Based Functionalizations of Nucleoside, Nucleotide and Nucleic Acids. *Curr. Org. Chem. 17*, 2164−2191.

(16) Sekhon, B. S. (2012) Click chemistry: current developments and applications in drug discovery. *J. Pharm. Educ. Res. 3*, 77−85.

(17) El-Sagheer, A. H., and Brown, T. (2010) Click chemistry with DNA. *Chem. Soc. Rev. 39*, 1388−1405.

(18) Xiong, H., Leonard, P., and Seela, F. (2012) Construction and Assembly of Branched Y-Shaped DNA: "Click" Chemistry Performed on Dendronized 8-Aza-7-deazaguanine Oligonucleotides. *Bioconjugate Chem. 23*, 856−870.

(19) Dyrager, C., Börjesson, K., Dinér, P., Elf, A., Albinsson, B., Wilhelmsson, L. M., and Grøtli, M. (2009) Synthesis and Photophysical Characterisation of Fluorescent 8-(1H-1,2,3-Triazol-4-yl)-adenosine Derivatives. *Eur. J. Org. Chem. 2009*, 1515−1521.

(20) Pujari, S. S., and Seela, F. (2013) Parallel Stranded DNA Stabilized with Internal Sugar Cross-Links: Synthesis and Click Ligation of Oligonucleotides Containing 2′-Propargylated Isoguanosine. *J. Org. Chem. 78*, 8545−8561.

(21) Berndl, S., Herzig, N., Kele, P., Lachmann, D., Li, X., Wolfbeis, O. S., and Wagenknecht, H. A. (2009) Comparison of a nucleosidic vs non-nucleosidic postsynthetic "click" modification of DNA with base-labile fluorescent probes. *Bioconjugate Chem. 20*, 558−564.

(22) Massi, A., Nuzzi, A., and Dondoni, A. (2007) Microwave-assisted organocatalytic anomerization of alpha-C-glycosylmethyl aldehydes and ketones. *J. Org. Chem. 72*, 10279−10282.

(23) Isobe, H., Fujino, T., Yamazaki, N., Guillot-Nieckowski, M., and Nakamura, E. (2008) Triazole-linked analogue of deoxyribonucleic acid ((TL)DNA): design, synthesis, and double-strand formation with natural DNA. *Org. Lett. 10*, 3729−3732.

(24) Sirivolu, V. R., Vernekar, S. K. V., Ilina, T., Myshakina, N. S., Parniak, M. A., and Wang, Z. (2013) Clicking 3′-Azidothymidine into Novel Potent Inhibitors of Human Immunodeficiency Virus. *J. Med. Chem. 56*, 8765−8780.

(25) Nuzzi, A., Massi, A., and Dondoni, A. (2007) Model Studies Toward the Synthesis of Thymidine Oligonucleotides with Triazole Internucleosidic Linkages Via Iterative Cu(I)-Promoted Azide−Alkyne Ligation Chemistry. *QSAR Comb. Sci. 26*, 1191−1199.

(26) Fujino, T., Yamazaki, N., and Isobe, H. (2009) Convergent synthesis of oligomers of triazole-linked DNA analogue (TLDNA) in solution phase. *Tetrahedron Lett.* 50, 4101−4103.

(27) Wu, J., Yu, W., Fu, L., He, W., Wang, Y., Chai, B., Song, C., and Chang, J. (2013) Design, synthesis, and biological evaluation of new 2′-deoxy-2′-fluoro-4′-triazole cytidine nucleosides as potent antiviral agents. *Eur. J. Med. Chem.* 63, 739−745.

(28) Santner, T., Hartl, M., Bister, K., and Micura, R. (2014) Efficient Access to 3′-Terminal Azide-Modified RNA for Inverse Click-Labeling Patterns. *Bioconjugate Chem.* 25, 188−195.

(29) Fomich, M. A., Kvach, M. V., Navakouski, M. J., Weise, C., Baranovsky, A. V., Korshun, V. A., and Shmanai, V. V. (2014) Azide phosphoramidite in direct synthesis of azide-modified oligonucleotides. *Org. Lett.* 16, 4590−4593.

(30) Krause, A., Hertl, A., Muttach, F., and Jäschke, A. (2014) Phosphine-Free Stille−Migita Chemistry for the Mild and Orthogonal Modification of DNA and RNA. *Chem.—Eur. J.* 20, 16613−16619.

(31) Fauster, K., Hartl, M., Santner, T., Aigner, M., Kreutz, C., Bister, K., Ennifar, E., and Micura, R. (2012) 2′-Azido RNA, a versatile tool for chemical biology: synthesis, X-ray structure, siRNA applications, click labeling. *ACS Chem. Biol.* 7, 581−589.

(32) Aigner, M., Hartl, M., Fauster, K., Steger, J., Bister, K., and Micura, R. (2011) Chemical Synthesis of Site-Specifically 2′-Azido-Modified RNA and Potential Applications for Bioconjugation and RNA Interference. *ChemBioChem* 12, 47−51.

(33) Beyer, C., and Wagenknecht, H.-A. (2010) In situ azide formation and ″click″ reaction of nile red with DNA as an alternative postsynthetic route. *Chem. Commun.* 46, 2230−2231.

(34) Wada, T., Mochizuki, A., Higashiya, S., Tsuruoka, H., Kawahara, S.-i., Ishikawa, M., and Sekine, M. (2001) Synthesis and properties of 2-azidodeoxyadenosine and its incorporation into oligodeoxynucleotides. *Tetrahedron Lett.* 42, 9215−9219.

(35) Padilla, R., and Sousa, R. (2002) A Y639F/H784A T7 RNA polymerase double mutant displays superior properties for synthesizing RNAs with non-canonical NTPs. *Nucleic Acids Res.* 30, e138.

(36) Weisbrod, S. H., and Marx, A. (2007) A nucleoside triphosphate for site-specific labelling of DNA by the Staudinger ligation. *Chem. Commun.*, 1828−1830.

(37) Weisbrod, S. H., Baccaro, A., and Marx, A. (2008) DNA Conjugation by Staudinger Ligation. *Nucleic Acids Symp. Ser.* 52, 383−384.

(38) Jawalekar, A. M., Meeuwenoord, N., Cremers, J. S., Overkleeft, H. S., van der Marel, G. A., Rutjes, F. P., and van Delft, F. L. (2008) Conjugation of nucleosides and oligonucleotides by [3 + 2] cycloaddition. *J. Org. Chem.* 73, 287−290.

(39) Jayaprakash, K. N., Peng, C. G., Butler, D., Varghese, J. P., Maier, M. A., Rajeev, K. G., and Manoharan, M. (2010) Non-nucleoside building blocks for copper-assisted and copper-free click chemistry for the efficient synthesis of RNA conjugates. *Org. Lett.* 12, 5410−5413.

(40) Suchy, M., Milne, M., Li, A. X., McVicar, N., Dodd, D. W., Bartha, R., and Hudson, R. H. E. (2011) Mono- and Tetraalkyne Modified Ligands and Their Eu³⁺ Complexes - Utilizing ″Click″ Chemistry to Expand the Scope of Conjugation Chemistry. *Eur. J. Org. Chem.*, 6532−6543.

(41) Gunji, H., and Vasella, A. (2000) Oligonucleosides with a nucleobase-including backbone- part 4: a convergent synthesis of ethynediyl-linked adenosine tetramers. *Helv. Chim. Acta* 83, 3229−3245.

(42) Cosyn, L., Palaniappan, K. K., Kim, S. K., Duong, H. T., Gao, Z. G., Jacobson, K. A., and Van Calenbergh, S. (2006) 2-Triazole-substituted adenosines: A new class of selective A(3) adenosine receptor agonists, partial agonists, and antagonists. *J. Med. Chem.* 49, 7373−7383.

(43) Gupte, A., Boshoff, H. I., Wilson, D. J., Neres, J., Labello, N. P., Somu, R. V., Xing, C. G., Barry, C. E., and Aldrich, C. C. (2008) Inhibition of Siderophore Biosynthesis by 2-Triazole Substituted Analogues of 5′-O-[N-(Salicyl)sulfamoyl]adenosine: Antibacterial

Nucleosides Effective against Mycobacterium tuberculosis. *J. Med. Chem.* 51, 7495−7507.

(44) Lakshman, M. K., Kumar, A., Balachandran, R., Day, B. W., Andrei, G., Snoeck, R., and Balzarini, J. (2012) Synthesis and Biological Properties of C-2 Triazolylinosine Derivatives. *J. Org. Chem.* 77, 5870−5883.

(45) Hong, V., Steinmetz, N. F., Manchester, M., and Finn, M. G. (2010) Labeling Live Cells by Copper-Catalyzed Alkyne−Azide Click Chemistry. *Bioconjugate Chem.* 21, 1912−1916.

(46) When this work was in progress [Zayas, J., Annoual, M., and Wnuk, S. F. (**2014**) Strain promoted click chemistry (SPAAC) of 8-azido purine and 5-azido pyrimidine nucleosides with cyclooctynes. *Abstr. Pap. Am. Chem. Soc.* 247, MEDI-301], Ito et al. reported an example of the SPAAC between the 8-azido-cAMP and a difluorinated cyclooctyne in HeLa cells: Ito, K., Liu, H., Komiyama, M., Hayashi, T., and Xu, Y. (2013) Direct Light-up of cAMP Derivatives in Living Cells by Click Reactions. *Molecules* 18, 12909−12915.

(47) Kumar, P., Hornum, M., Nielsen, L. J., Enderlin, G., Andersen, N. K., Len, C., Hervé, G., Sartori, G., and Nielsen, P. (2014) High-Affinity RNA Targeting by Oligonucleotides Displaying Aromatic Stacking and Amino Groups in the Major Groove. Comparison of Triazoles and Phenyl Substituents. *J. Org. Chem.* 79, 2854−2863.

(48) Gourdain, S., Martinez, A., Petermann, C., Harakat, D., and Clivio, P. (2009) Unraveling the photochemistry of the 5-azido-2′-deoxyuridine photoaffinity label. *J. Org. Chem.* 74, 6885−6887.

(49) Neef, A. B., and Luedtke, N. W. (2014) An azide-modified nucleoside for metabolic labeling of DNA. *ChemBioChem* 15, 789−793.

(50) Marks, I. S., Kang, J. S., Jones, B. T., Landmark, K. J., Cleland, A. J., and Taton, T. A. (2011) Strain-Promoted "Click" Chemistry for Terminal Labeling of DNA. *Bioconjugate Chem.* 22, 1259−1263.

(51) Shelbourne, M., Chen, X., Brown, T., and El-Sagheer, A. H. (2011) Fast copper-free click DNA ligation by the ring-strain promoted alkyne-azide cycloaddition reaction. *Chem. Commun.* 47, 6257−6259.

(52) Singh, I., Freeman, C., and Heaney, F. (2011) Efficient Synthesis of DNA Conjugates by Strain-Promoted Azide-Cyclooctyne Cycloaddition in the Solid Phase. *Eur. J. Org. Chem.* 2011, 6739−6746.

(53) Singh, I., Freeman, C., Madder, A., Vyle, J. S., and Heaney, F. (2012) Fast RNA conjugations on solid phase by strain-promoted cycloadditions. *Org. Biomol. Chem.* 10, 6633−6639.

(54) Other approaches including the click reaction between norbornenes and nitrile oxides for the modification of oligonucleotides have also been developed; see: Gutsmiedl, K., Wirges, C. T., Ehmke, V., and Carell, T. (2009) Copper-Free "Click" Modification of DNA via Nitrile Oxide−Norbornene 1,3-Dipolar Cycloaddition. *Org. Lett.* 11, 2405−2408.

(55) Zimmet, J., Järlebark, L., Hammarberg, T., Van Galen, P. J. M., Jacobson, K. A., and Heilbronn, E. (1993) Synthesis and Biological Activity of Novel 2-Thio Derivatives of ATP. *Nucleosides Nucleotides* 12, 1−20.

(56) Sinkeldam, R. W., Greco, N. J., and Tor, Y. (2010) Fluorescent Analogs of Biomolecular Building Blocks: Design, Properties, and Applications. *Chem. Rev.* 110, 2579−2619.

(57) Ranasinghe, R. T., and Brown, T. (2005) Fluorescence based strategies for genetic analysis. *Chem. Commun.*, 5487−5502.

(58) Tanpure, A. A., Pawar, M. G., and Srivatsan, S. G. (2013) Fluorescent Nucleoside Analogs: Probes for Investigating Nucleic Acid Structure and Function. *Isr. J. Chem.* 53, 366−378.

(59) Holmes, R. E., and Robins, R. K. (1965) Purine nucleosides. IX. The synthesis of 9-β-D-ribofuranosyluric acid and other related 8-substituted purine ribonucleosides. *J. Am. Chem. Soc.* 87, 1772−1776.

(60) Stewart, J. A., Wilson, C. J., and Swarts, B. M. (2014) Effect of Azide Position on the Rate of Azido Glucose−Cyclooctyne Cycloaddition. *J. Carbohydr. Chem.* 33, 408−419.

(61) Chattopadhyaya, J. B., and Reese, C. B. (1977) Reaction between 8-Bromoadenosine and Amines - Chemistry of 8-Hydrazinoadenosine. *Synthesis*, 725−726.

(62) Buenger, G. S., and Nair, V. (1990) Dideoxygenated purine nucleosides substituted at the 8-position: chemical synthesis and stability. *Synthesis*, 962–966.

(63) Kuzmin, A., Poloukhtine, A., Wolfert, M. A., and Popik, V. V. (2010) Surface Functionalization Using Catalyst-Free Azide-Alkyne Cycloaddition. *Bioconjugate Chem. 21*, 2076–2085.

(64) Schultz, M. K., Parameswarappa, S. G., and Pigge, F. C. (2010) Synthesis of a DOTA–biotin conjugate for radionuclide chelation via Cu-free click chemistry. *Org. Lett. 12*, 2398–2401.

(65) Tworowska, I., Sims-Mourtada, J., and Delpassand, E. S. International Patent Application WO 2012/177701 A2, USA, 2012.

(66) Chenoweth, K., Chenoweth, D., and Goddard, W. A. (2009) Cyclooctyne-based reagents for uncatalyzed click chemistry: A computational survey. *Org. Biomol. Chem. 7*, 5255–5258.

(67) Saenger, W. (1984) *Principles of Nucleic Acid Structure*, Springer, New York.

(68) Ikehara, M., Uesugi, S., and Yoshida, K. (1972) Nucleosides and nucleotides. XLVII. Conformation of purine mucleosides and their 5'-phosphates. *Biochemistry 11*, 830–836.

(69) Sarma, R. H., Lee, C.-H., Evans, F. E., Yathindra, N., and Sundaralingam, M. (1974) Probing the interrelation between the glycosyl torsion, sugar pucker, and the backbone conformation in C(8) substituted adenine nucleotides by proton and proton-phosphorus-31 fast Fourier transfer nuclear magnetic resonance methods and conformational energy calculations. *J. Am. Chem. Soc. 96*, 7337–7348.

(70) Gourdain, S., Petermann, C., Harakat, D., and Clivio, P. (2010) Highly efficient and facile synthesis of 5-azido-2'-deoxyuridine. *Nucleosides, Nucleotides Nucleic Acids 29*, 542–546.

(71) Rayala, R., and Wnuk, S. F. (2012) Bromination at C-5 of pyrimidine and C-8 of purine nucleosides with 1,3-dibromo-5,5-dimethylhydantoin. *Tetrahedron Lett. 53*, 3333–3336.

(72) Sletten, E. M., and Bertozzi, C. R. (2008) A hydrophilic azacyclooctyne for Cu-free click chemistry. *Org. Lett. 10*, 3097–3099.

(73) Sun, K. M., McLaughlin, C. K., Lantero, D. R., and Manderville, R. A. (2007) Biomarkers for phenol carcinogen exposure act as pH-sensing fluorescent probes. *J. Am. Chem. Soc. 129*, 1894–1895.

(74) Andréasson, J., Holmén, A., and Albinsson, B. (1999) The Photophysical Properties of the Adenine Chromophore. *J. Phys. Chem. B 103*, 9782–9789.

(75) Daniels, M., and Hauswirth, W. (1971) Fluorescence of the Purine and Pyrimidine Bases of the Nucleic Acids in Neutral Aqueous Solution at 300 K. *Science 171*, 675–677.

(76) Nir, E., Kleinermanns, K., Grace, L., and de Vries, M. S. (2001) On the Photochemistry of Purine Nucleobases. *J. Phys. Chem. A 105*, 5106–5110.

(77) Noé, M. S., Ríos, A. C., and Tor, Y. (2012) Design, Synthesis, and Spectroscopic Properties of Extended and Fused Pyrrolo-dC and Pyrrolo-C Analogs. *Org. Lett. 14*, 3150–3153.

(78) O'Mahony, G., Ehrman, E., and Grøtli, M. (2008) Synthesis and photophysical properties of novel cyclonucleosides—substituent effects on fluorescence emission. *Tetrahedron 64*, 7151–7158.

(79) Manderville, R. A., Omumi, A., Rankin, K. M., Wilson, K. A., Millen, A. L., and Wetmore, S. D. (2012) Fluorescent C-Linked C-8-Aryl-guanine Probe for Distinguishing syn from anti Structures in Duplex DNA. *Chem. Res. Toxicol. 25*, 1271–1280.

(80) Rankin, K. M., Sproviero, M., Rankin, K., Sharma, P., Wetmore, S. D., and Manderville, R. A. (2012) C8-Heteroaryl-2'-deoxyguanosine Adducts as Conformational Fluorescent Probes in the NarI Recognition Sequence. *J. Org. Chem. 77*, 10498–10508.

(81) Striker, G., Subramaniam, V., Seidel, C. A. M., and Volkmer, A. (1999) Photochromicity and fluorescence lifetimes of green fluorescent protein. *J. Phys. Chem. B 103*, 8612–8617.

(82) Wohnsland, F., and Faller, B. (2001) High-Throughput Permeability pH Profile and High-Throughput Alkane/Water log P with Artificial Membranes. *J. Med. Chem. 44*, 923–930.

(83) Kansy, M., Senner, F., and Gubernator, K. (1998) Physicochemical High Throughput Screening: Parallel Artificial Membrane Permeation Assay in the Description of Passive Absorption Processes. *J. Med. Chem. 41*, 1007–1010.

(84) Sugano, K., Nabuchi, Y., Machida, M., and Aso, Y. (2003) Prediction of human intestinal permeability using artificial membrane permeability. *Int. J. Pharm. 257*, 245–251.

(85) Fujikawa, M., Nakao, K., Shimizu, R., and Akamatsu, M. (2007) QSAR study on permeability of hydrophobic compounds with artificial membranes. *Biorg. Med. Chem. 15*, 3756–3767.

(86) Fujikawa, M., Ano, R., Nakao, K., Shimizu, R., and Akamatsu, M. (2005) Relationships between structure and high-throughput screening permeability of diverse drugs with artificial membranes: Application to prediction of Caco-2 cell permeability. *Biorg. Med. Chem. 13*, 4721–4732.

(87) Molina-Arcas, M., Casado, F. J., and Pastor-Anglada, M. (2009) Nucleoside transporter proteins. *Curr. Vasc. Pharmacol. 7*, 426–434.

(88) Lee, J., Twomey, M., Machado, C., Gomez, G., Doshi, M., Gesquiere, A. J., and Moon, J. H. (2013) Caveolae-Mediated Endocytosis of Conjugated Polymer Nanoparticles. *Macromol. Biosci. 13*, 913–920.

(89) Berezin, M. Y., and Achilefu, S. (2010) Fluorescence Lifetime Measurements and Biological Imaging. *Chem. Rev. 110*, 2641–2684.

(90) Seksek, O., and Bolard, J. (1996) Nuclear pH gradient in mammalian cells revealed by laser microspectrofluorimetry. *J. Cell Sci. 109*, 257–262.

(91) Yoo, H., Yang, J., Yousef, A., Wasielewski, M. R., and Kim, D. (2010) Excimer formation dynamics of intramolecular pi-stacked perylenediimides probed by single-molecule fluorescence spectroscopy. *J. Am. Chem. Soc. 132*, 3939–3944.

(92) Islam, M. S., Honma, M., Nakabayashi, T., Kinjo, M., and Ohta, N. (2013) pH Dependence of the Fluorescence Lifetime of FAD in Solution and in Cells. *Int. J. Mol. Sci. 14*, 1952–1963.

(93) Haga, Y., Ishii, K., Hibino, K., Sako, Y., Ito, Y., Taniguchi, N., and Suzuki, T. (2012) Visualizing specific protein glycoforms by transmembrane fluorescence resonance energy transfer. *Nat. Commun. 3*, 907–913.

(94) Schaeffer, H. J., and Thomas, H. J. (1958) Synthesis of potential anticancer agents. XIV. Ribosides of 2,6-disubstituted purines. *J. Am. Chem. Soc. 80*, 3738–3742.

(95) Eaton, D. F. (1988) Reference Materials for Fluorescence Measurement. *Pure Appl. Chem. 60*, 1107–1114.

(96) Lukavenko, O. N., Eltsov, S. V., Grigorovich, A. V., and McHedlov-Petrossyan, N. O. (2009) Solubility and fluorescence lifetime of 2,5-diphenyloxazole and 1,4-bis(5-phenyl-oxazolyl-2)-benzene in water–ethanol and water–acetone solvent systems. *J. Mol. Liq. 145*, 167–172.